The effect of enniatin B and beauvercin – two novel feed contaminants in the intestinal barrier of Atlantic salmon (*Salmo salar*)

Åsne Omdal

Master of Science in Biology - Environmental toxicology

Department of biological Sciences, University of Bergen

Institute of marine research

June 2022

Supervisor: Kai K. Lie, Institute of Marine Research

Co-supervisor: Øystein Sæle, Institute of Marine Research

The effect of enniatin B and beauvercin – two novel feed contaminants in the intestinal barrier of Atlantic salmon (*Salmo salar*)

Åsne Omdal

Master of Science in Biology - Environmental toxicology

Department of biological Sciences, University of Bergen

Institute of Marine Research

June 2022

Supervisor: Kai K. Lie, Institute of Marine Research

Co-supervisor: Øystein Sæle, Institute of Marine Research

Acknowledgements

The work in this thesis was performed at The Institute of Marine Research (IMR). I would like to thank to my main supervisor Kai K. Lie for excellent guidance and for always answering all my questions. Your patience, encouragement and knowledge is highly appreciated. Thanks to co-supervisor Øystein Sæle for guidance through the intestines. Also, a thanks to Marc Berntssen for answering questions when I come knocking on your door. Additionally, a big thanks to Hui-Shang Tung for complete training in the lab and to Sofie Søderstrøm for sharing your expertise in this field.

A huge appreciation to my family for the support and the funding of my snack budget during this period. And of course a big thanks to friends, boyfriend and fellow students for many unforgettable memories.

Table of contents

Abstract

In the recent years there has been a shift towards replacing the marine proteins in Atlantic salmon *(Salmo salar)* feed with a bigger share of plant-based products. This also introduces novel contaminants like mycotoxins. Mycotoxins are secondary metabolites from fungi, which can arise either in the field or through storage. According to surveillance, the prevalence of the two structurally related mycotoxins enniatin B (EnnB) and beauvericin (Bea) in Norwegian salmon feed were especially high. Despite these high levels, the knowledge of toxic potential of EnnB and Bea in regards of fish welfare and absorption, metabolism and distribution in salmon is lacking. In addition to no risk management of dietary levels of EnnB and Bea, results in potentially exposing Atlantic salmon to high levels of these toxins.

In this study, the effects of orally ingested EnnB and Bea in Atlantic salmon were investigated through a sub chronic (3 month) exposure study. The concentrations were 0.25 mg/kg, 5 mg/kg and 80 m/g for EnnB and 0.25 mg/kg, 5 mg/kg and 25 mg/kg for Bea. The intestinal permeability in the distal intestine of salmon high dose EnnB and Bea was investigated, using the gut sac model. Furthermore, classic histology was preformed of distal intestinal segments of high dose EnnB and Bea. In addition to gene expression (RT-qPCR) with biomarkers related to intestinal structure, inflammation and disruption of cellular metabolism.

The permeability results showed that low and high dose Bea significantly increased the permeability, while no effect was seen in EnnB. The histological assessment revealed no signs of inflammation or disturbed intestinal structure. Furthermore, low dose Bea significantly upregulated the expression of *ALAS1* and *Gpx4.* EnnB on the other side, significantly upregulated the expression *SOCS2* in the low dose and *MnSOD* was upregulated in the high dose. In conclusion this could be to the ionophoric characteristics of these two mycotoxins. While the difference in results could be attributed to their minor but meaningful dissimilarities, resulting in a different degree of toxicity. Underlining the importance of further *in vivo* characterization of EnnB and Bea, to be able to set safe dietary levels in salmon feed.

1. Introduction

1.1 Perspective

Aquaculture production plays a critical part in addressing the demands of the world's ever-increasing human food consumption (Pahlow et al., 2015). Both in Norway and the rest of the world, the Atlantic salmon (*Salmo salar)* is one of the most significant aquaculture species. Norway hosts the largest population of wild and farmed Atlantic salmon and is hence the main supplier of salmon all over the world (Liu et al., 2011). During the last decades there has been a shift towards incorporating a larger part of plant-based ingredients to replace marine proteins and lipids in salmon feed, as seen in Figure 1.

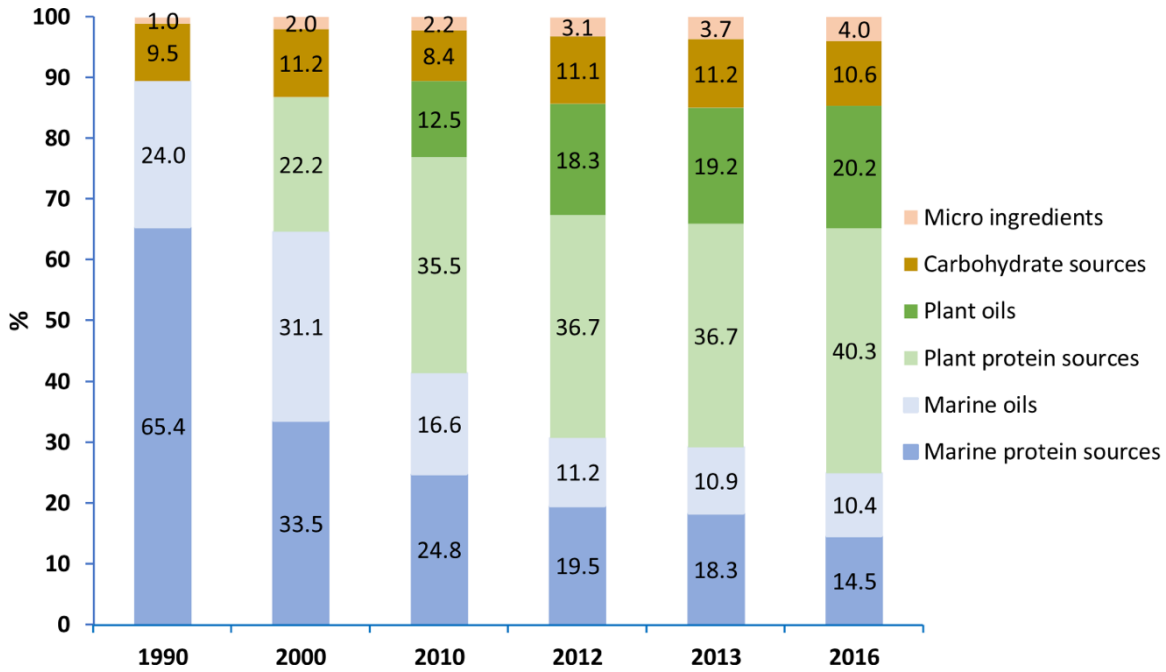

Figure 1: The shift towards a more plant-based feed content (%) in Norwegian salmon feed from from 1990 to 2016. Graph published by Aas et al. (2019).

Changing the feed composition by incorporating a bigger share of plant based ingredients is beneficial from an economic and sustainable point of view (Aas et al., 2019). The introduction of these new feed components has also introduced ”novel” contaminants, i.e. emerging, such as pesticides and mycotoxins that previously has not been associated with farming marine carnivorous fish (Berntssen et al., 2021).

1.2 Occurrence of mycotoxins

Mycotoxins occur all over the world and are usually formed either during growth or during storage. Due to their chemical and thermal stability, they can get carried over to processed foods and are therefore common contaminators (Liew and Mohd-Redzwan, 2018, Anfossi et al., 2016). Emerging mycotoxins are mostly found in raw materials like wheat and maize, and in finished feed (Human, 2019). Countries like Brazil, Argentina and parts of Asia have a high prevalence of mycotoxins and are the largest agri-food exporters (Human, 2019). An explanation could be that these areas are also regarded as hotspots for impact of climate change. The Norwegian producers of salmonid feed import 100% of their vegetable feed components due to economic advantages (Bernhoft et al., 2013). Resulting in an important pathway for introducing contaminants like mycotoxins to aquaculture.

A global survey performed by BIOMIN Research Centre in Australia has shown that climate and weather impact the occurrence of mycotoxins (Gruber-Dorninger et al., 2019). The growth of the fungi itself varies geographically, differing on which conditions are favorable for the certain species (Anfossi et al., 2016). The occurrence of both fungi, hence mycotoxins, are expected to increase the upcoming years as a result of climate change. Making of both risk assessment and management of mycotoxins essential in the close future (Marroquín-Cardona et al., 2014)

1.3 Directive of mycotoxins

The regulation of mycotoxins with maximum levels and guidance values varies from country to country (Anfossi et al., 2016). The European union (EU) provides legislative regulation with both guidance- and maximum levels of mycotoxins, based on recommendations from international risk-assessment bodies like European Food Safety Authority (EFSA) and JECFA (the expert committee of World Health Organization/Food and Agriculture Organization of the United Nations). The risk management- and legislative body in Norway is the Norwegian Food Safety Authority (Mattilsynet). Guidance values provided by EU are implemented in the Norwegian legislation, as a result of Norway being a member of EEA (European Economic Area) (Norwegian Food Safety Authority, 2020). The Norwegian Food safety authority can also request the Norwegian Scientific committee for food and environment (VKM) to perform independent risk assessment. In 2013 VKM presented a thorough risk assessment regarding

mycotoxins in Norwegian grains (Bernhoft et al., 2013). The Norwegian veterinary institute did a review of the guidance values presented by this risk assessment, which was also supported by the National Institute of Feed, Nutrition and Seafood research (NIFES) (Norwegian Food Safety Authority, 2019).

The Institute of Marine Research (IMR) are also conducting research on request from the Norwegian Food Safety authority. IMR performs an annual monitoring program on behalf of the Norwegian Food Safety authority, to get an overview of already known and new potential risk factors regarding public health, animal welfare and environment (Institute of Marine Research, 2021). In 2020 there were no values exceeding the established guidance values of contaminants or additives in feed or feedstuff. For the time being the guidance values are only recommendations, based on type of feed and animal species. Whereas deoxynivalenol, ochratoxin A, T-2 and HT-2 (trichothecenes), zearalenone and fumonisins are species with guidance values (Norwegian Food Safety Authority, 2019). Aflatoxin is the exception which obtains an absolute guidance value due to carcinogenic properties (Norwegian Food Safety Authority, 2019). In the three last years, the monitoring program has also included enniatins and beauvericin (Bea) due to an observed high prevalence in feed (Institute of Marine Research, 2021). Regarding mycotoxins in general, there is not yet enough data and knowledge related to the potential effects to preform correct risk management and establish absolute maximum levels in food and feed (Liew and Mohd-Redzwan, 2018).

1.4 Fusarium genus

The *fusarium* genus includes a broad range of fungi which can produce both harmless and toxic secondary metabolites (Maranghi et al., 2018). *Fusarium* most commonly infect cereals, causing both diseases and wilt to several parts of a plant and species (Jonsson, 2017). For fusarium to grow, water is essential. At least 20% water content is needed for fusarium to grow on grains. The fungi are aerobe and CO_2 inhibit its growth. Several of the species can grow at lower temperature and they are mainly growing in the fields but can also continue growing until the water content falls below 20% (Norwegian Food Safety Authority, 2019). Important groups of *fusarium* toxins are trichothecenes, zearalenone and fumonisins. Within

these groups there are many sub-families of toxins which functions in diverse ways and has various adverse effects (Escrivá et al., 2015).

Trichothecenes are the largest sub-group and are divided into an A- and B group. An example within the B group is deoxynivalenol (DON) which is produced by several fungi, including *fusarium graminearum, F. culmorum.* DON is present in cereals and grains, particularly in wheat. Its' adverse effects include irregular growth, immunity and intestinal barrier for mammals, poultry, carp and Atlantic salmon (*Salmo salar)* (Moldal et al., 2018). The A – group within trichothecenes include T2 and TH2-toxins. These are produced by several *fusarium* species in cereal grains including wheat, maize, corn, rice, beans and soya. The ability to inhibit protein-synthesis is most likely the source of their toxicity. At higher doses, T2 and HT-2 can inhibit RNA and DNA synthesis (Bertero et al., 2018). The wide fusarium genus also produce less known metabolites like enniatins and Bea (Prosperini et al., 2017).

Enniatin

Amongst the group of enniatins, enniatin B (EnnB) is one of the most prevalent and reported as a natural contaminant in Europe (Prosperini et al., 2017). Surveillance conducted by the Institute of Marine Research (IMR) on behalf of the Norwegian Food Safety Authority, have reported EnnB of having the highest prevalence amongst enniatins in formulated fish feed in Norway (Institute of Marine Research, 2021).

F. avenaceum, F. proliferatum, F. tricinctum, and *F. chlamydosporum* are common EnnB producers, and in rare cases *trichothecene* – producing strains (Jonsson, 2017). EnnB is synthesized from a non-ribosomal multienzyme named enniatin synthetase, which is coded from the gene esyn1 (Jonsson, 2017). It is a lipophilic compound with a characteristic cyclic hexadepsipeptide structure as seen in Figure 2, with peptide- and ester bonds connecting the subunits together (Krug et al., 2018). It has free electron pairs acting as nucleophiles which enables the molecule to establish interactions to cations (Bertero et al., 2018).

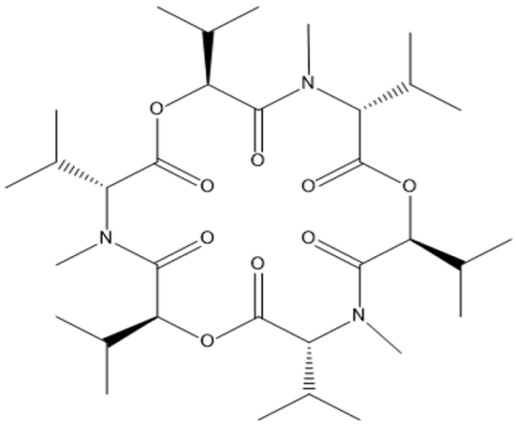

Figure 2: Chemical structure of Enniatin B. Modified from (Prosperini et al., 2017). Created with ChemDraw.

These interactions with cations are weak and can happen either 1:1 or 2:1, where two EnnB are connected to one cation forming a 'sandwich structure' resembling a disk. This sandwich structure creates a lipophilic exterior with a polar interior, enabling the molecule to penetrate biological membranes rapid and extensively (Krug et al., 2018, Tedjiotsop Feudjio et al., 2010). As a result, they can effortlessly reach the systemic circulation (Krug et al., 2018).

The molecule also has hydrophilic and hydrophobic functional groups attached onto it (Tedjiotsop Feudjio et al., 2010). The capability of both hydrophobic and hydrophilic interactions also allows EnnB to get incorporated into lipid bilayers of cell membranes, functioning as selective pores thus increasing permeability of alkali cations. Thus, the proposed mechanism of actions is acting as an ionophore, possibly altering intra and extra-cellular environment (Bertero et al., 2018). Which in turn could result in damaging levels of reactive oxygen species (ROS) (Søderstrøm et al., 2022). The functional group for EnnB is N-methylvaline (Tedjiotsop Feudjio et al., 2010).

Despite EnnB being a commonly present mycotoxin in feed, its toxic properties and adverse effects are yet to be fully characterized. Research preformed on enniatin's *in vitro* for several cell lines has shown insecticidal, antibacterial, anti-fungal and cytotoxic effects, but there is very low proven toxicity *in vivo* (Krug et al., 2018, Jonsson, 2017). According to Jonsson et. al (2017) an explanation for low toxicity *in vivo* could be rapid biotransformation in the organism. The few *in vivo* studies that have been published has been on terrestrial mammals and poultry, and none on aquatic animals. To produce more data regarding toxicity on Bea and EnnB, EFSA in 2018 performed a subacute exposure experiment, both *in vitro* and *in vivo* oral genotoxicity-testing in addition to repeated dose oral toxicity study of mice. The duration of exposure was at most 3 days. The results yielded different outcomes for the two substances, generating a No Observed Adverse Effect Level (NOAEL) of 0.18 mg/kg body weight (BW) for female mice and 1.8 mg/kg BW for male mice (Maranghi et al., 2018).

Beauvericin

As seen in Figure 3, Bea is structurally related to EnnB. This gives Bea the same interactions with cations in either 1:1 or 2:1 complexes, creating a lipophilic exterior enabling it to cross biological membranes (Jonsson, 2017). It is produced by beauvericin synthetase and the amino acid in Bea is L-phenylalanine (Tedjiotsop Feudjio et al., 2010). Bea is less studied than EnnB, as it has not been detected to the same extent as EnnB.

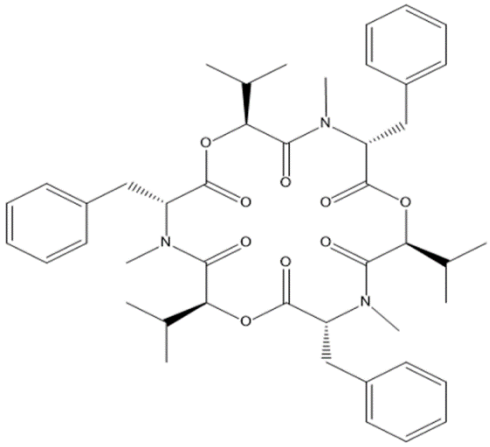

Figure 3: Chemical structure of beauvericin. Modified from (Santini et al., 2012). Created with ChemDraw.

Beas mechanism of action is proposed to be similar to EnnB, structural resemblances (Bertero et al., 2018). Previous research on both Bea and EnnB has mainly been done on animals like chicken, pigs and other terrestrial animals as these species are traditionally fed on feed which could contain high levels of mycotoxins. To this date there are none published *in vivo* studies on the effect of Bea or EnnB in fish. Based on both *in vitro* and *in vivo data*, Bea NOAEL was set by EFSA at 0.1 mg/kg body weight BW per day for female mice, and 1 mg/kg BW for male mice (Maranghi et al., 2018).

1.5 Mycotoxin toxicity and occurrence

Mycotoxins are secondary metabolites that have toxic properties and are produced by fungi and moulds. Mycotoxins arise from diverse genus and species, functioning in various ways. Different mycotoxins-classes are penicillium toxins, ochratoxins, *fusarium* toxins, aflatoxins and patulin (Anfossi et al., 2016). Ingestion is the most common route of exposure, in addition to less common routes like dermal contact and inhalation. The toxic infliction to human and animals is called mycotoxicosis (Liew and Mohd-Redzwan, 2018). Possible adverse effects of exposure are dependent on the duration, species of mycotoxin and species sensitivity (Liew and Mohd-Redzwan, 2018). However, one of the proposed main mechanisms of the major mycotoxins is oxidative stress. Oxidative stress refers to overproduction of reactive oxygen species (ROS) leading an imbalance of oxidants and antioxidants. The implications of oxidative

stress can be DNA damage, altered lipid peroxidation, damaged proteins and possibly cell death (Da Silva et al., 2018).

The aflatoxins (AFs) are the most often detected mycotoxin in human- and animal feed, and hence the most researched. AFs are produced by molds like *Aspergillus flavs* and *Aspergillus parasiticus* (Burcham, 2014). AF_1 has potent hepatocarcinogen effects in mammals (Liew and Mohd-Redzwan, 2018). Its occurrence is mostly related to hot and tropic climates like Africa, middle and South America and Asia. In Norway AFs are found associated with imported grains from these areas. For Norwegian crops, ochratoxin A and *fusarium* toxins are the most important mycotoxins. The two groups arise through storage fungi (*ochratoxin A*) and from field fungi (*fusarium*) (Norwegian Food Safety Authority, 2019).

1.6 Metabolism and detoxification

The toxicity of xenobiotics in general depends on how it is absorbed, distributed, metabolized and excreted by an animal. When metabolized in the liver, the xenobiotic will go through two phases of biotransformation where the main goal is to increase hydrophilicity for easy excretion out of the organism (Burcham, 2014). Phase I consist of oxidation, reduction or hydrolysis reaction and phase II consist of conjugation reactions. The pathway of detoxification depends on the characteristics of the xenobiotic (Gad, 2007). However, this process can also lead to bioactivation of a molecule which increases its toxicity. Inflammation caused by mycotoxins is determined by the toxic potential of the mother compound and its metabolites. AlfatoxinB_1 is a mycotoxin which have been proven to be bioactivated though conjugation in phase II of the metabolism (Burcham, 2014). As mentioned, resulting in a carcinogenic metabolite.

The biotransformation of EnnB and Bea on the other hand, is still rather unknown. Research has however suggested the possibility of EnnB and Bea to enter the enterohepatic circulation (Rodríguez-Carrasco et al., 2016, Søderstrøm et al., 2022). The enterohepatic circulation is a process where molecules, drugs or other substances, are transported from the liver to the bile. The bile, together with other molecules, will then be transported to the intestine where it will get absorbed by the enterocytes to exert its function followed by transportation back to the liver (Roberts et al., 2002).

1.7 Physiology of Atlantic salmon

The Atlantic salmon is an anadrome species, which involves a period of starvation when it sexually matures and migrate up rivers to spawn (Løkka et al., 2013). Anadrome species have the ability to adapt to saltwater and freshwater, by pumping Na+ and Cl ions against their surrounding concentration gradient (McCormick, 2012). It is also categorized as a carnivorous teleost fish, which has a gastrointestinal system differing from mammals. Teleost intestine in general vary in length, degree of looping, size of pyloric area and whether a stomach is present or not. The intestine is generally divided into fore-, mid- and hindgut, but there is little literature on intestine morphology thus standardization of the different sections can be unclear (Løkka et al., 2013).

The intestine is where absorption of nutrients happens, but also the first barrier of protection. There are four levels of barriers protecting the intestine against toxins, as illustrated in Figure 4 (Gao et al., 2020). The first barrier is the microbial barrier, consisting of gut microbiota in the lumen of the intestine. The gut microbiota has many functions where some are degradation of macromolecules, nutrient absorption and synthesis of proteins (Guerre, 2020). The mucus layer acts as a chemical barrier lining the intestinal epithelium. It is important in protecting the intestinal epithelium from making direct contact with the luminal content. This is done through mucines and peptides secreted by goblet cells (Nimalan et al., 2022). The physical barrier is the actual epithelium. The epithelial cells are semipermeable and interconnected by tight junctions (TJ) (Gao et al., 2020). Typical TJ-proteins are claudins, occludins and tricellulin. The tight junctions regulate the paracellular transport and if disrupted, could cause influx of toxins affecting the microbiota resulting in inflammation (McLaughlin et al., 2009). Serval types of immune cells within lamina propria makes out the immunological barrier (Gao et al., 2020). It is in the intestine potential mycotoxins exert their toxicity, possibly altering one of these barriers in addition to changing in the histomorphology of the intestine (Liew and Mohd-Redzwan, 2018).

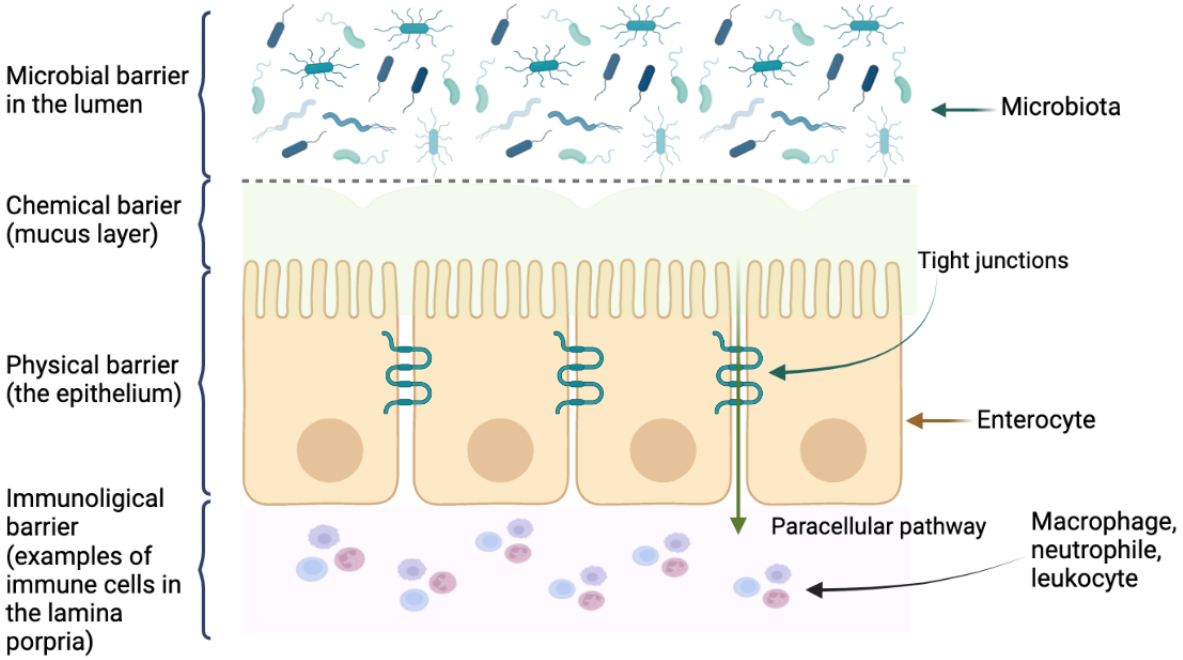

Figure 4. Simplified illustration of the four intestinal barriers in normal homeostasis. Microbiota in the lumen acting as a microbial barrier. In addition to the chemical barrier of the mucus layer protecting the intestinal epithelium from making direct contact with the lumen. Furthermore, the epithelium acting as the physical barrier. The adjacent enterocytes in the epithelium are interconnected by tight junctions. Underneath the epithelium is the immunological barrier. The immunological barrier consists of several immune cells. The examples of immune cells in this simplified figure are macrophages, neutrophiles and leukocytes. Modifies from (Gao et al., 2020). Created with Biorender.com.

The research that already has been conducted regarding mycotoxicosis has mostly been done through acute exposure experiments. But as exposure to mycotoxins are through ingestion, low doses over time could cause chronic toxicity (Escrivá et al., 2015). Additionally, mycotoxins are often found to co-occur, as fungi can produce several types of mycotoxins (and its derivatives) (Jonsson, 2017). The concurrency of components can result in interactive effects causing in higher, equal or lower toxicity compared to the effects of the individual components (Burcham, 2014). The interaction-effects of mycotoxins are categorized as synergistic, additive and antagonistic (Gao et al., 2020). Closer research of deoxynivalenol and zearalenone has shown synergistic and additive effects. Some adverse effects has been documented to be direct and indirect pro-inflammatory effect, in addition to aggravating inflammation (Gajęcka et al., 2013).

1.8 The gut matters in aquaculture

Intestinal health is an increasing focus in aquaculture. An efficient utilization of feed is the key to keep costs low and still produce optimal and robust fish, which is the main goal when it comes to farming of fish (Nimalan et al., 2022). A criteria for making this happen is a well-functioning intestine, which ensures absorption of nutrients and regulation of physiological processes, in addition to playing a comprehensive part in the fish immune system. There has been a lot of intestinal difficulties in aquaculture and the context is often not very clear. Research has shown that feed-components and additives, as well as environmental factors, affect the mucous barrier of the intestine resulting in sub optimal health and welfare (Sørensen et al., 2021). In light of the above, the Norwegian seafood research fund (FHF) allocated funds over 18 M NOK in 2017 to enhance the knowledge of salmon intestinal health, feed composition and possible solutions to gut health challenges (Norwegian Seafood Research Fund, 2017)

1.9 Aim of study

To this date there are no recommended guidance values regarding the two emerging mycotoxins EnnB and Bea. The scarce amount of research that already has been conducted, on terrestrial farm animals, indicates that the two toxins negatively affect animals' physiology, further influencing animal welfare. As marine feedstuff is increasingly being replaced by alternative plant-based feed components, the emergence of mycotoxins constitutes an increasing threat to fish health and welfare. The hypothesis is that long term oral exposure of EnnB and Bea will disrupt intestinal integrity and permeability of the distal intestine, in addition to upregulate biomarkers related to disruption of intestinal integrity. This study aims to contribute to relevant statistically significant data regarding the effect of mycotoxins EnnB and Bea of intestinal integrity and thereby welfare of Atlantic salmon. The three main objectives of this study by exposing EnnB and Bea to Atlantic salmon are;

I. Performing classic histopathology to investigate possible disruption of distal intestinal integrity.

II. Ex vivo intestinal leakage essay to assess permeability in the distal intestine.

III. Examine if any biomarkers related to intestinal integrity and metabolic state was upregulated as a result of treatment.

2. Material and method

2.1 Feeding trial

This trial was planned as a sub-chronic toxicological dose-response experiment and conducted at the Institute of Marine Research (IMR) in Matre (Matredal, Norway; 60°52'N, 05°35'E) from 14.09.2021 to 02.12.2021. Prior to start of the trial (17.08.2021) all fish were individually pit-tagged, weighed and measured. Following, the fish were randomly distributed for acclimatization into 21 tanks (3 tanks pr treatment), allocating 39 individuals per tank. During the acclimatization period (4 weeks) only basal feed was given. During the entire trial the fish were kept in tanks with flow through-system with freshwater at a stable temperature of 12 C°. The tubs were size 95x95x40 cm of ca 300 L. The fish density of fish at trial start was 10 kg/m^3.

There were in total seven different feeding groups. Three groups with different concentrations of each mycotoxin in addition one shared control group. The low, medium and high levels were respectively 0.25 mg/kg, 5 mg/kg, and 25 mg/kg for Bea and 0.25 mg/kg, 5 mg/kg, and 80 mg/kg for EnnB, as seen in Table 1. Each of the seven groups were fed in triplicates (n = 3).

After acclimation, as of 14.09.2021 the control group were given basal feed only and the other groups were in triplicates put on a diet enriched with EnnB or Bea for 12 weeks. During the trial there was supposed to be in total 3 samplings, at start, mid and end of trial. The end sampling was however divided into two, due to running out of experimental feed (EnnB only). The start sampling was at t=0 and mid sampling at = 6 weeks of exposure. The end $sampling_1$ for EnnB exposed groups was at t=10 weeks and end $sampling_2$ for Bea exposed groups at t=12 weeks of exposure. To ensure animal welfare throughout the trial period, several measures were taken. Daily supervision was done by technical personnel at the research station, as described in the FOTS application (ID 26017). The reader is referred to the appendix for complete description of kits, chemicals, software and instruments utilized in this thesis,

2.2 Experimental diets

The experiment included seven different feeding groups. All the feed-ingredients were screened for EnnB and Bea prior to basal feed production to ensure no misleading values. Predicted limiting factors were also considered when designing the feed, to ensure no effect on performance of the fish. Synthetically produced pure EnnB or Bea was added to basal feed in low, medium and high concentrations (Table 1) by personnel at IMR, followed by top coating.

The levels of mycotoxins used in this trial were chosen based on reported levels in commercial feed from surveillance, in addition to data from in vitro and force-feeding trials done by IMR. The levels of EnnB were higher compared to Bea due to higher background levels of EnnB found in feedstuff, in addition to a higher sensitivity towards Bea shown in *in vitro* cytotoxicity test of salmon (Søderstrøm et al., 2022, Institute of Marine Research, 2021). Both mycotoxins had a shared exposure level of 5mg/kg at medium concentration.

Table 1. Nominal concentrations of beauvericin and enniatin B added to feed

Dose	Beauvericin (mg/kg)	Enniatin B (mg/kg)
Low	0.25	0.25
Medium	5	5
High	25	80

2.3 Calculation of performance parameters and BMDL

Several parameters were measured and calculated throughout the trial. The body weight (BW) in grams and fork length (L) in centimeters of each individual was measured at start-, mid- and end of trial. These data were applied to calculate the Fulton's condition factor (CF) at each time point as described by Fjelldal et al. (2006), $\mathrm{CF} = 100 * \frac{BW}{L^3}$. The specific length rate (SLR) and specific growth rate (SGR) was calculated based on the collected data from start (day 0) to the end of trial period (day 79 for Bea or 68 for EnnB). SLR reflecting the increase of fork length in percent per day ($\frac{(\ln \text{Final L} - \ln \text{Initial L})}{\text{Experimental period (days)}} * 100$), and SGR reflecting the increase of bodyweight (BW) in percent per day ($\frac{(\ln \text{Final BW} - \ln \text{Initial BW})}{\text{Experimental period (days)}} * 100$) (Fjelldal et al., 2006) .

The feed conversion ratio (FCR) displaying the feed efficiency based on feed intake and BW gain per tank, through $\frac{\text{Feed intake (g)}}{\text{BW gain (g)}}$. EFSA's online model was utilized to calculate the benchmark dose level (BMDL) (EFSA Scientific Committee, 2017). EFSA now uses this approach rather than NOAEL and LOAEL. This is due to BMD accounting for statistical limitations better than previously used NOAEL. The BMDL – approach uses statistical and mathematical modeling to fit the best curve to the data within the observed range. Using lower 95% confidence interval to account for uncertainties. The lower benchmark response level was set to 10% response and derived a corresponding benchmark dose.

2.4 Sampling

Due to assumed high metabolization-degree of EnnB and Bea, there were no starvation-period and all fish were fed pre-sampling. Different stations with assigned takes of which tissue to sample was planned in advance.

The samplings were divided into two different days. Each individual were given specific LIMS numbers. During sampling all fish were individually weighed and 6 fish per tank were randomly selected. The fish were euthanized by overdose of Tricaine Pharmaq MS-222 (40mgx5) followed by blow to head. The sampling of intestinal tissue was standardized to a size of approximately 2 mm thickness, as seen in (Figure 5). The first distal-intestine incision was made approximately 2 cm from the end of the colon being allocated to histology analyses (Figure 5). The tissue samples for histology analysis were preserved in plastic histology cassettes and fixated in 4% paraformaldehyde solution for approximately 24 hours and then transferred to 70 % ethanol solution for further storage. The mid-tissue sample of the distal intestine was allocated to RNA extraction and qPCR, while the last intestinal tissue sample was allocated to other analyzes not presented in this trial (Figure 5). These two samples were stored in 2ml cryogenic vials preserved in liquid nitrogen.

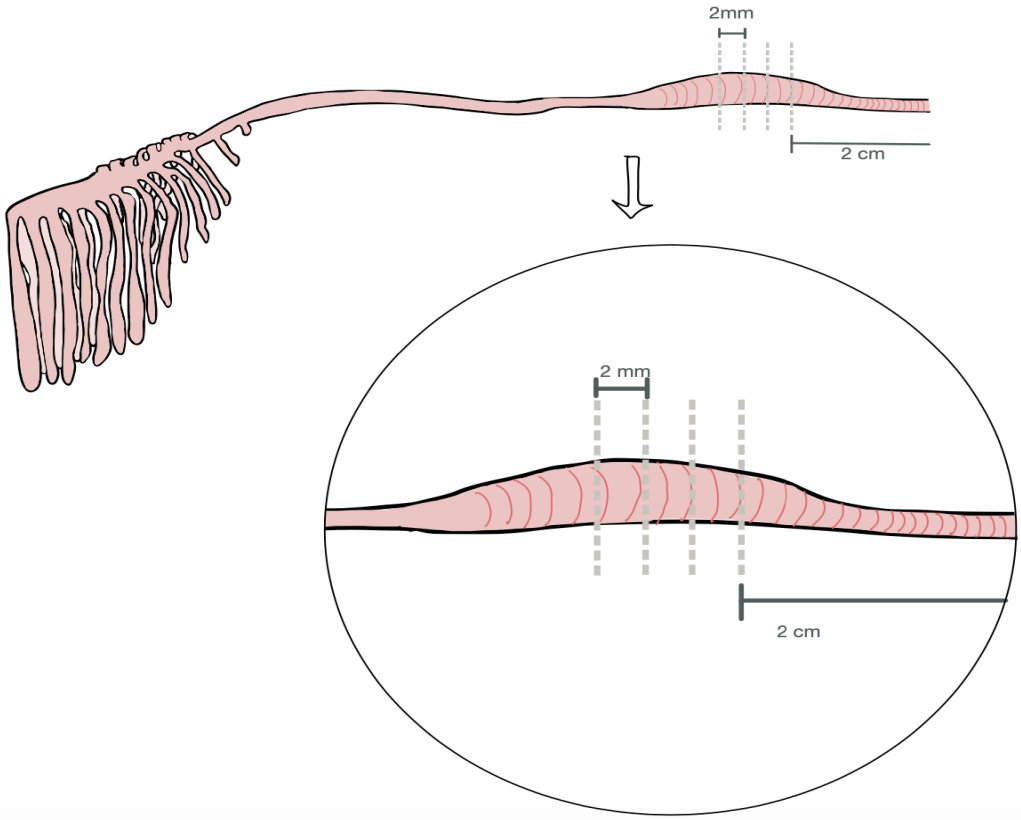

Figure 5. Illustration of the distal intestine in Atlantic salmon *(Salmo Salar*) and the standardized position of the different samples. Depicting the locations and size of the incisions cut at the distal intestine. Illustration created using iPadPro and the application Notability (v10.6).

2.5 Histology

2.5.1 Resin casting

The tissue samples stored on 70% ethanol were further dehydrated in 80% ethanol solution for one hour, then transferred to 96% ethanol for one hour as the final dehydration step. Technovit 7100 Kit was used to embed the tissue samples in hydrophilic resin casts. The basic solution of Technovit 7100 was mixed 50/50 with 96% ethanol, constituting a pre-infiltration solution. The tissue samples were transferred to this pre-infiltration solution for approximately 2 hours. The infiltration solution was prepared by adding Technovit 7100 hardener 1 (1g) to the basic Technovit 7100 solution (15 mL). The tissue samples were then submerged in the infiltration solution for approximately 24 hours. The following day, polymerization solution was prepared by mixing the infiltration solution (unused) with Technovit 7100 hardener 2. The prepared tissue-samples were positioned horizontally in the histoform embedding cavities. 6 samples per block. Roughly 3 ml polymerization solution was added to histology molds. Histoblocks were carefully placed on top of the molds, with purpose

of attaching to the casting blocks and preventing oxygen from inhibiting the hardening process. Polymerization transpired over the next hours.

2.5.2 Sectioning

In advance of sectioning, an incision was made at the top left corner in the casting block to distinguish the orientation of the blocks. The hardened casting blocks were then sectioned using Leica RM2165 microtome with mounted disposable blades TC-65 (Leica). The trimming was done at a setting of 8-10 mm. Once the blocks were adequately trimmed, displaying a uniform cut of the imbedded tissue, 3 mm thin sections were made. The sections were immediately transferred to a bowl of deionized water to unfold the sections, giving a better overview of shape and suitability for histology analyses. The chosen sections were put on control slides, placed on top of a slide warmer SW85 of 40 C° to evaporate the water preparing the sections for staining.

2.5.2 Staining

Toluidine Blue Stain for plastic sections was prepared in fume hood by dissolving 1g sodium borate in 100mL deionized water. This was followed by adding of 1g stain powder Toluidine Blue (Appendix B, Table B1). The solution was stirred until it dissolved and then filtered. Furthermore, the control slides were submerged in the staining solution for approximately 2 minutes and heated on slide warmer SW85 (Leica). Once the slides dried, excess stain was rinsed off with running water. The slides were then placed back on the slide warmer until dried. Cooled and dried slides were then coverslipped using Entellan® mounting medium.

All prepared slides were roughly reviewed using Nikon Eclipse E200 microscope at 10x and 40x magnification. The most suitable slides were selected for further evaluations. The selected slides were then scanned and converted to digital images using NanoZoomer® S60 at 40x magnification. The produced digital images were closer analyzed in the compatible image viewing software, NDP®.view2. The length of all representative intestinal folds was measured using the ruler-tool in NDP®.view2 and exported to Excel (v2022). The measurements were standardized to range from *muscularis mucosae* to the brush boarder at the apical end of the fold (Figure 6).

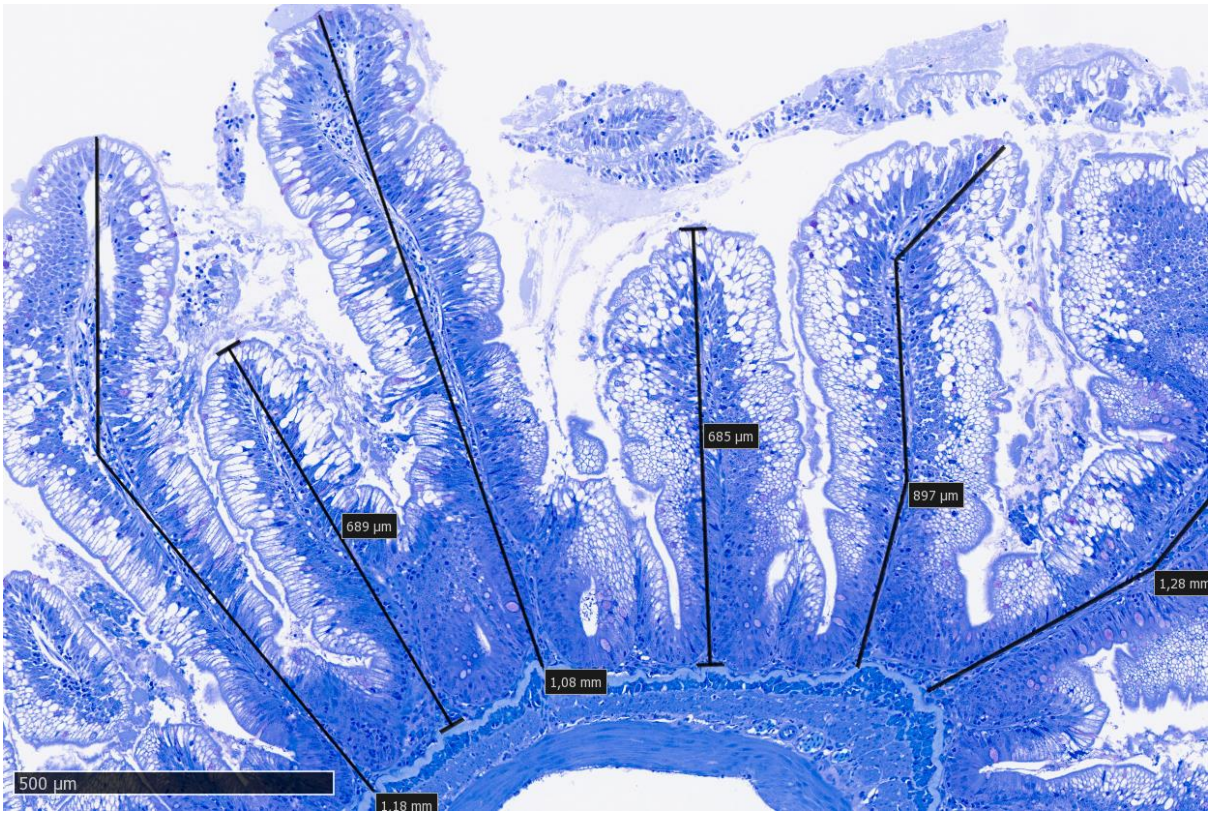

Figure 6. Measurement-illustration of distal intestinal folds in Atlantic salmon (*Salmo salar*). The measurements were standardized to range from *muscularis mucosae* to the brush boarder at the apical end of the folds, as in demonstrated by the black lines. Scalebar = 500 µm. Image produced in NDP®.view.2

2.6 Ex vivo intestinal leakage

This assay was preformed inspired by (Mateer et al., 2016). It was conducted at two occasions: the end-sampling$_1$ for the EnnB-exposed groups and two weeks later at the end-sampling$_2$ for the Bea-exposed groups. Minor practical improvements were done at end-sampling$_2$.

Ringers' solution (Appendix B, Table B7) was prepared in advance of assay. Additionally, 10 mg of the fluorescein isothiocyanate-dextran marker (Appendix B, Table B8) was dissolved in 20 mL ringers' solution (Appendix B, Table B7). 4 fish per tank (per feeding group) were used in this gut sac model. The temperature bath was turned on and temperature was stabilized to approximately 12 °C. Hoses connected to valves was mounted to an oxygen tank containing 99.7 % O_2 and 0.3 % CO_2, ensuring continuous supply. Needles were attached at the tip of the hoses and positioned at the bottom of each glass tube. 10 mL ringers' solution was added per tube. A dark cover (garbage bag) was placed on top of the setup to minimize light exposure. A dilutional series was created and utilized as standard curve for the FITC-D molecule

(fluorescein Isothiocyanate-dextran). The standard curve was made in a linear scale, by diluting stock solution of FITC-D with ringers´ solution.

The fish were euthanized by blow to head, to minimize potential biological and chemical stress-responses in the animal. A horizontal incision was cut in the middle of the abdomen. Intestines were dissected and the hindgut section were excised and visceral fat was carefully removed using tweezer and scalpel. The average length and width of the segments was respectively 3,4 cm ± 0,7 and 1,3 cm ± 1,2. The intestinal segment was then cleansed by carefully flushing out the luminal content in a posterior direction, using a1000 µl pipette and ringer solution. The distal opening of the intestinal segments was tied together using dental floss. At the other end, a pre-tied loop was placed over the opening and a 300 µl pipette was used to insert the dissolved FITC-D marker (0.5mg/mL). The inserted amount of FITC-D was adjusted to each individual, 1 µl per gram of bodyweight.

The valves connected to the oxygen hoses were used to adjust the oxygen-flow to an adequate amount, preventing over-bubbling and loss of ringers' volume in the tubes, as illustrated in Figure 7. The prepared intestinal segment was transferred to the designated tube and submerged in the 10 mL ringer's solution. Paper clips was used to position the intestines vertically. This procedure was done for each segment and time of submerging was noted. The buffer in the glass tubes were sampled in triplicates (100 µl) in 20-minute intervals, for the next three hours. Ringers' solution removed during continuous sampling (300 µl), volume was replaced with fresh ringers' solution (300 µl) at each interval. The samples were put in 96 well-plates, which were covered in aluminum foil and stored in fridge℃. After completing the experimental period, each intestinal segment was cut open to measure length and width using a ruler.

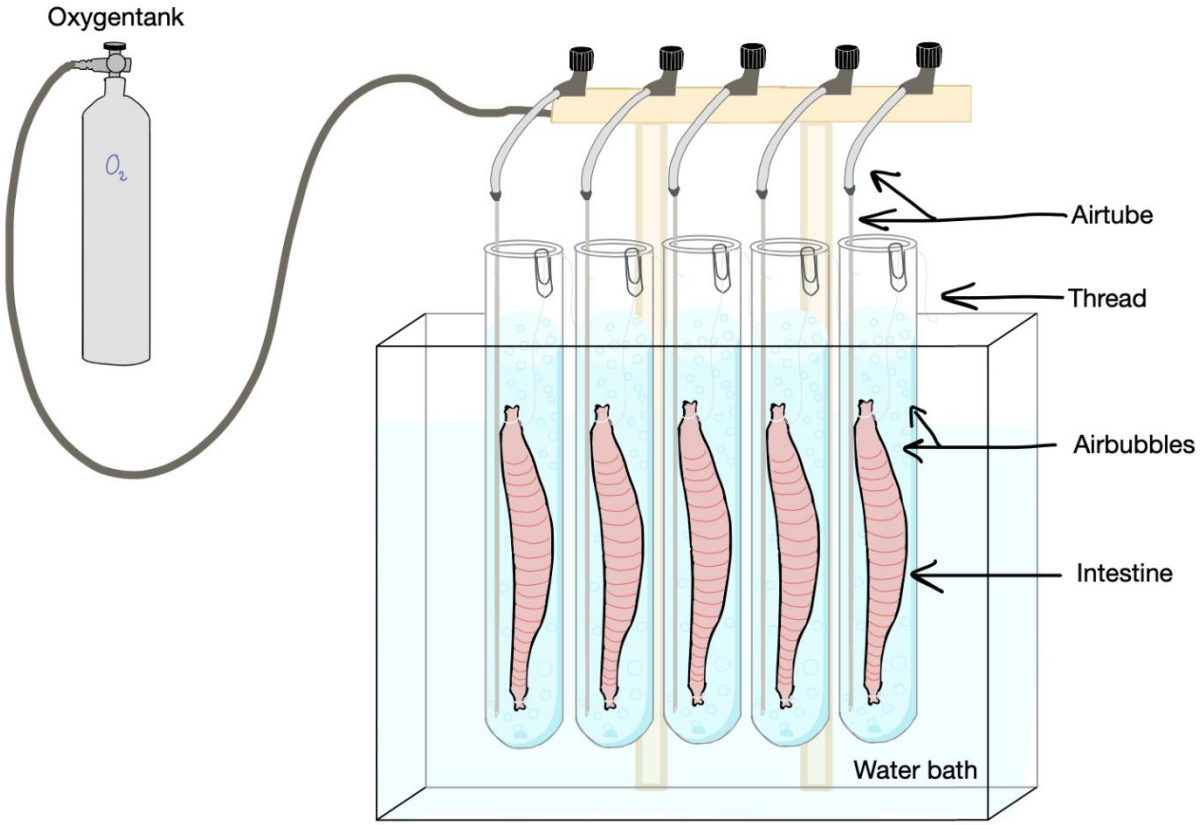

Figure 7. Illustration of the ex vivo intestinal leakage setup. Distal intestinal segments of Atlantic salmon *(Salmo salar)* submerged in 10 mL ringers' solution in tubes. All tubes were immersed in a temperature-regulated water bath. Each tube getting continuous supply of oxygen trough tubes from connected to oxygen tank, also shown by the air bubbles. The amount of oxygen flow was regulated by individual vales for each tube. The intestinal segments were positioned a vertical position by a thread attached to paperclips at the top of the tube. Illustration created using iPadPro and the application Notability (v10.6).

2.6.1 Analysis of samples

The plates containing the samples and standards were centrifuged for one minute at 1000 rpm before further analysis. To detect the amount of fluorescence of FITC-D in each sample and the standards, PerkinElmer's Victor X5 Multilabel plate reader was used. The plates were measured at excitation wavelength 493 nm and emission wavelength of 518 nm. The registered FITC-D counts were further processed by calculating the cumulative concentration of each time point (Qt), plotting Qt versus time (minutes), and thereby obtaining the slope ($\delta Q/\delta t$), as illustrated in Figure 8. From this, it was possible to calculate the apparent permeability through dividing the slope by the area of tissue x initial concentration of FITC-D.

Equations for calculations presented below.

$Qt = (C_t * V_r) + (Q_t\ sum * V_s)$

Q_t = Cumulative concentration at time t
C_t = Concentration at time t
V_r = Volume at receiver side
$Q_{t\ sum}$ = Sum of all previous Q_t
V_s = Volume sampled

$P_{app} = (\delta Q/\delta t)/(A * C_0)$

$\delta Q/\delta t$ = Slope
A = Area of tissue
C_0 = Initial concentration

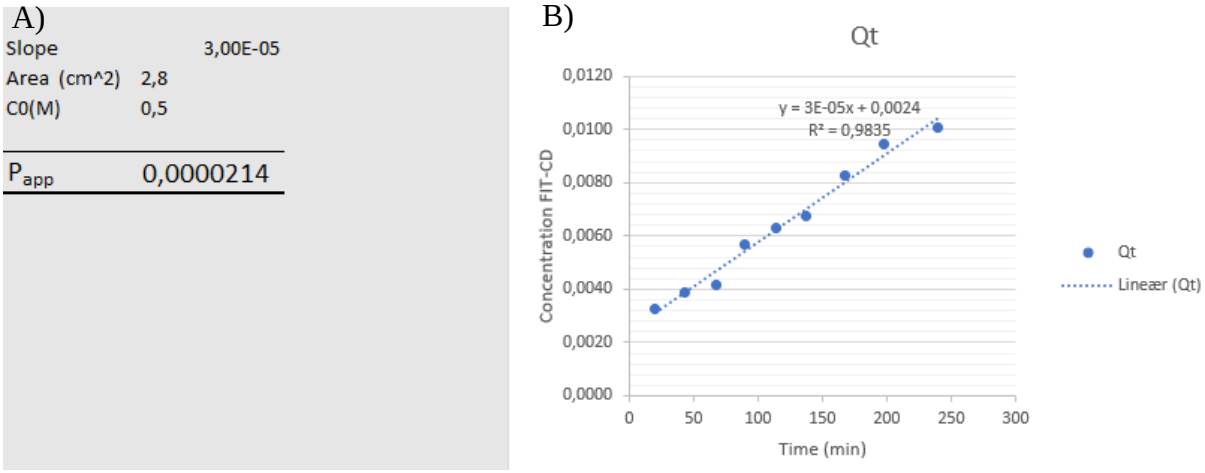

Figure 8. A representative example where B) the cumulative concentration (Qt) of fluorescein isothiocyanate–dextran (FITC-D) in the y-axis is plotted versus the sampling timepoints in the x-axis, and A) the slope of the linear graph is extracted to calculate the apparent permeability by dividing the slope on (the area of distal intestinal segment (cm^2)) *(initial concentration of FITC-D).

2.7 Quantitative PCR

2.7.1. OneStep RT-PCR

To control the specificity of possible primers PCR was preformed, using Qiagen OneStep RT-PCR kit. Primers were diluted with TE buffer to a concentration of 50 µM. All reagents were thawed and kept on ice, apart from the enzyme mix which was kept on -20°C freezing block. A mix consisting of 3 µl from all samples was diluted to a concentration of approximately 0,6 µg RNA. The shared reagents (Appendix B, Table B2) were mixed in one tube, except the enzyme mix. The shared-reagents mix was allocated into individual tubes, then primers and enzyme mix were added. The tubes were spun down and a RT PCR reaction (specified Appendix B, Table B2) was preformed using T100 Thermal Cycler. For gel electrophoresis, a 1% agarose gel was made in 100 ml 0,5 x TAE runningbuffer. The solution was heated in a

microwave until it dissolved, cooled in room temperature and 10 µl GelRed Nucleic Acid Stain was added. After 1 hour the gel was stiffened and the well-comb was removed. 3 µl X10 Blue Juice loading buffer was added to each sample tube (containing 25 µl) and mixed well. 6 µl Gel Pilot 50 bp ladder was used as standard and 10 µl sample tube was allocated to individual wells. The electrophoresis was run for 4 minutes at 80V to properly attach the contents to well. The volt was reduced to 60V and run for approximately 1,5 hours. The gel was then depicted using ChemiDoc™ XRS+ System and Image Lab TM 6.0.1 software.

2.7.2 Testing primers on dilution series

Primers chosen based on the results obtained from One Step RT-PCR were further analyzed by preforming qPCR on a dilution series made in triplicates. The melting cure was analyzed in CFX Maestro. The primers that displayed a Cq value below Cq = 28 in addition to a single peak melting curve were selected for further analyses (Table 2).

Table 2. Primer sequences for qPCR analysis

Gene	Forward (5'-3')	Reverse (5'-3')	Amplicon size (bp)
ALAS1_2	CCCCATATCAGCTCACGCAT	CTCAGCTTTGGGACAGTCGT	149
ARP	GAAAATCATCCAATTGCTGGATG	CTTCCCACGCAAGGACAGA	106
ATP8	CCTCCTAAAGTACTCGGCCA	GGTCAGTTTCAGGGTTCAGG	86
CLDN25b	CCTGTAAGAGGGGTCCATCAR	TGACACATGTTCTGCCCTGT	101
GADD45	TGAAGCAGCAAAATCATTGAATG	TGCCTGGATCAGGGTGAAGT	118
Occludin	GACAGTGAGTTCCCCACCATR	ATCTCTCCCTGCAGGTCCTT	91
PCNA	TGAGCTCGTCGGGTATCTCT	GTCCTCATTCCCAGCACACT	170
SOCS1_1	TTCTTGATCCGGGATAGTCG	TGTTTCCTGCACAGTTCCTG	239
B-actin	CCAAAGCCAACAGGGAGAA	AGGGACAACACTGCCTGGAT	91
EF1ab	CACTGCCAACGAAGCCAAAGAGAT	CAAACTGCTTCAGCTTGGGCTTGA	247
rpl	CCAATGTACAGCGCCTGAAA	CGTGGCCATCTTGAGTTCCT	110

2.7.3 RNA extraction

RNA was extracted from the intestinal tissue-samples according to the EZ1 protocol (Quiagen), using BioRobot EZ1 and RNA 6000 Nano kit. The samples were randomly selected, two from

each treatment group, providing n = 6. The samples were kept on dry ice to prevent degradation of RNA. The segment-size had to be reduced to approximately 100g. This was done using a scalpel. Once the correct size, the sample was transferred to precellystubes containing 750 µl Qiazol and 3 zirconium beads. The samples were then homogenized using Precellys® 24 homogenizer at 6000 rpm for 3 x 15 seconds. The homogenized samples were added 150 µl chloroform and incubated for 3 minutes at room temperature (rm) before being centrifuged at 4 °C and 12 000 for 15 minutes. In the meantime, BioRobot EZ1 and EZ1 RNA Tissue Mini Kit was prepared according to the producer's protocol. When centrifugation was completed, 350 µl of the upper water phase was transferred to 2 ml sample tubes and 10 µl DNase was added to each sample. The tubes were then placed in the designated position in the BioRobot EZ1 and protocol for 50 µl elution of RNA samples was performed.

2.7.4 Validation of RNA quality and integrity

After completed RNA extraction, concentration and purity of RNA of each sample was measured using NanoDrop. Purity exhibited in A_{260}/A_{280}- and A_{260}/A_{230}-ratios, which were 2,10 ± 0,04 and 2,31 ± 0,04, respectively. Bioanalyzer and RNA 6000 Nano LabChip Kit was used to further analyze 12 randomly selected samples to evaluate RNA integrity. All reagents were incubated in rm for 30 minutes before usage. RNA samples were denatured using a heating block at 70 °C for 2 minutes. RNA Nano dye was vortexed for 10 seconds and spinned down and 0,5 µl was added to 32.5 gel aliquot. This gel-dye mix was then centrifuged at 13 000 x g for 10 minutes. New Eppendorf tubes were prepared and 2 µl RNA was added to each tube, obtaining a concentration between 100-500 ng/µl. Chip priming station was put in position C and RNA Nano chip was mounted. 9 µl gel dye-mix, 5 µl RNA marker and RNA Ladder was added to its' designated wells, according to producers' protocol. 1 µl RNA samples were also added to wells (1-12). BioAnalyzer was turned on and cleaned according to producers' protocol. The Nanochip was centrifuged at 2400 rpm for 1 minute and then immediately positioned in BioAnalyzer. The software 2100 Expert was connected to BioAnalyzer to perform Eucaryote Total RNA Nano SerieII assay. Duration of assay was approximately 30 minutes. Integrity was measured to be 6,85±0,5. After completed assay, the instrument was cleaned according to producer protocol.

2.7.5 cDNA

For each sample, RNA were diluted using milli-Q water to achieve a concentration value within 50 ng/µl ± 2.5 %. The final concentration was checked using NanoDrop and further adjusted until within wanted concentration. 3 µl from each sample was collected in a new tube and used to make a dilution series with concentrations of 100, 50, 25, 12.5, 6.25 and 3.125 ng/µl. These concentrations were confirmed using NanoDrop. 40 µl of reaction mix (Appendix B, Table B3) were added each well of the 96-well plate. 10 µl of RNA and 10 µl of the dilution series was individually added in triplicates to separate wells (technical replicates). Two negative controls were also added to the plate. Nac (negative amplification control) containing 40 µl reaction mix (without Multiscribe enzyme) + 10 µl of the 50 ng/µl point in dilution series. The second negative control was Ntc (negative template control) containing 40 µl reaction mix + 10 µl milli-Q water. The plate was covered and centrifuged at 50 x g for 1 minute. cDNA synthesis (reverse transcriptase) was then preformed using T100 Thermal Cycler applying program specified in (Appendix B, Table B4). After completed protocol, the cDNA plate was centrifuged for 1 minute at 1200 x g and stored at -20 °C until further use.

2.7.6 qPCR

The cDNA plate and all reagents were thawed on ice. Afterwards, the cDNA plate was centrifuged at 1000 x g for 1 minute followed by 1:1 dilution (50 µl) with milli Q water using Biomek 4000 pipetting robot. The cDNA plate was then centrifuged at 1000 x g for 1 minute followed by vortexing at 1300 rpm for 15 minutes and then transferred to ice. A reaction mix (Appendix B, Table B5). was prepared for each of the primers, and aliquoted to 8-strips tubes, 110 µl per tube. The reaction mix, the cDNA plate and a 384-well real time plate was placed in the pipetting robot, pipetting 2 µl sample and 8 µl reaction mix into real time plate. When the program was completed, the real time plate was enclosed with optical adhesive cover and centrifuged for 2 minutes at 15000 x g. The Light Cycler 480 instrument was turned on and the RT-PCR reaction conditions listed in Appendix B, Table B6 was chosen.

The obtained data was initially processed in CFX Maestro where the amplification of genes was controlled. As there was observed high variation in standard deviations (std. dev.) amongst several measurements, a reference point of std. dev ≤ 0.2 was set for all samples to minimize uncertainties. Sample number 2021-1030/154 (Plate 1 - well F17) and 2021-

1030/276 (Plate 2 - well N6) was read as N/A. All qPCR data was then transferred into Excel, where the Quantity value was calculated based on the amplification factor for each gene. The amplification factor (E) was obtained through the equation of PCR kinetics; $E = N_{C+1}/N_C$ which reflects the increase in amplicon per cycle (Ruijter et al., 2009). The VBA Microsoft excel geNorm macro (Vandesompele et al., 2002), was utilized to calculate a normalization factor based on the three reference genes, *rpl*, *B-actin* and *Efa1*. The target genes were then normalized and transferred to GraphPad Prism for statistical analysis.

2.7.7 Data editing and statistics

All the statistical analyses in this thesis were performed in GraphPad Prism (version 9.3.0). One-way analysis of variance (ANOVA) was performed on the measured fold-length of histology samples. The apparent permeability of each intestinal sac and the normalized gene expression was tested *by* conducing Kruskal-Wallis One-Way ANOVA followed by Dunnett's multiple comparisons post hoc test. The significance of treatment in performance parameters was tested by One-way nested ANOVA, where treatment group was the categoric factor and individuals (random effect) were nested into tanks (random effect).

3. Results

3.1 General health

No mortalities were observed during the acclimatization period or experimental period in any of the dietary treatment groups. The control group maintained a normal physique. Some morphological changes were observed in high dose enniatin and high dose beauvericin exposed groups. Both EnnB and Bea exposed fish had a significantly reduced specific growth rate (SGR) with increased exposure levels from start to end, and mid to end of trial as seen in Table 3 and Table 4. Increased Bea levels refer to concentrations of 0.25, 0.5 and 25 mg/kg respectively, and increased EnnB concentrations refer to concentrations of 0.25, 0.5 and 80 mg/kg respectively. The individuals exposed to high dose Bea gradually developed a more slender form as seen from a reduced CF at the end of trial, day 76 (Table 3). The enniatin exposure resulted in a more dense body shape as seen from the reduced length growth both mid to end of trial (day 32-68) and start to end of the trial (0-68), while the condition factor was not affected at end of trial (day 68) (Table 4). All individuals were x-rayed and analyzed by Per Gunnar Fjelldal (IMR, Matredal 2021) after completed trial, which confirmed bone deformities in the high dose enniatin group at end of trial (day 68).

Table 3. Significant length rate and significant growth rate for control and beauvericin treatment groups from mid to end (day 32-76) and start to end (day0-76) of trial. Condition factor for control and beauvericin at day end of trial (day 76). BEA1, BEA2 and BEA3 represent concentrations of 0.25, 0.5 and 25 mg/kg respectively. Significance tested by One-way nested ANOVA. * $p < 0.05$, ** $p < 0.005$, *** $p < 0.0001$, ns = non-significant.

	Control		BEA1		BEA2		BEA3		
	mean	sd	mean	sd	mean	sd	mean	sd	
Significant length rate:									
Day 32-76	3.82	0.93	3.91	0.58	3.95	0.83	3.75	0.91	ns
Day 0-76	3.84	0.66	3.83	0.50	3.73	0.49	3.71	0.53	ns
Significant growth rate:									
Day 32-76	1.05	0.15	1.11	0.13	1.09	±	0.74	0.12	*
Day 0-76	1.10	0.14	1.04	0.09	0.99	±	0.86	0.08	*
Condition factor:									
Day 76	1.20	0.10	1.23	0.09	1.21	0.13	1.09	0.10	***

Table 4. Significant length rate and significant growth rate for control and enniatinB treatment groups from mid to end (day 32-68) and start to end (day 0-68) of trial. Condition factor for control and beauvericin at day end of trial (day 68). ENN1, ENN2 and ENN3 represent concentrations of 0.25, 0.5 and 80 mg/kg respectively. Significance tested by One-way nested ANOVA. * $p < 0.05$, ** $p < 0.005$, *** $p < 0.0001$, ns = non-significant.

	Control		ENN1		ENN2		ENN3		
	mean	sd	mean	sd	mean	sd	mean	sd	
Significant length rate:									
Day 32-68	3.61	± 0.56	3.75	± 0.56	2.79	± 0.47	2.52	± 0.68	**
Day 0-68	3.81	± 0.40	3.71	± 0.49	3.29	± 0.52	3.30	± 0.59	***
Significant growth rate:									
Day 32-68	0.95	± 0.17	0.98	± 0.11	0.72	± 0.14	0.68	± 0.17	***
Day 0-68	1.13	± 0.13	1.07	± 0.13	0.93	± 0.16	0.99	± 0.19	**
Condition factor:									
Day 68	1.20	± 0.10	1.211	± 0.08	1.22	± 0.09	1.21	± 0.12	ns

3.2 Feed intake and feed conversion

Fish fed elevated Bea levels had significantly increased feed intake from mid to end of trial (day 32-76), as seen in Table 5. The elevated Bea levels refer to concentrations of 0.25, 0.5 and 25 mg/kg respectively. Also, a significantly increased FCR observed in both mid to end (day 32-76) and start to end of trial (day 0-76). The feed intake from start to end of trial remained unaffected by Bea treatment. Exposure to elevated EnnB level did not significantly affect feed intake or FCR form mid to end (32-68 days) or start to end (0-68 days) of trial, as seen in Table 6. Where elevated EnnB concentrations refer to concentrations of 0.25, 0.5 and 80 mg/kg respectively. Significance of feed intake and FCR was tested by One-way ANOVA due to summarized tank-based data.

Table 5. Tank-based data for food conversion ratio and feed intake of control and beauvericin treatment groups during mid to end of trial (32-72 days) and start to end of trial (0-76). BEA1, BEA2 and BEA3 represent concentrations of 0.25, 0.5 and 25 mg/kg respectively. Significant tested by One-way ANOVA. * $p < 0.05$, ** $p < 0.005$. ns=non-significant

	Control	BEA1	BEA2	BEA3	
	mean sd	mean sd	mean sd	mean sd	
Feed intake:					
Day 32-76	1.13 ± 0.02	1.16 ± 0.02	1.24 ± 0.06	1.22 ± 0.02	*
Day 0 -76	1.20 ± 002	1.23 ± 0.03	1.27 ± 0.02	1.26 ± 0.02	ns
Feed convertion ratio:					
Day 32-76	1.08 ± 0.02	1.10 ± 0.05	1.38 ± 0.05	1.69 ± 0.15	*
Day 0 -76	1.01 ± 0.02	1.07 ± 0.02	1.22 ± 0.07	1.26 ± 0.08	**

Table 6. Tank-based data for food conversion ratio and feed intake for ennitainB exposed groups during mid to end of trial (32-68 days) and start to end of trial (0-68). ENN1, ENN2 and ENN3 represent concentrations of 0.25, 0.5 and 80 mg/kg respectively. The food conversion ratio and feed intake of the control group differs slightly in period, where start to end of trial is 0-67 days, and mid to end of trial is 32-76. Tested by One-way ANOVA. ns=non-significant

	Control		ENN1	ENN2	ENN3	
	mean sd		mean sd	mean sd	mean sd	
Feed intake:						
Day 32-76	1.13 ± 0.02	Day 32-68	1.06 ± 0.09	1.06 ± 0.11	1.01 ± 0.10	ns
Day 0 -76	1.20 ± 0.02	Day 0 -68	1.01 ± 0.01	0.99 ± 0.03	0.97 ± 0.02	ns
Food convertion ratio:						
Day 32-76	1.08 ± 0.02	Day 32-68	1.14 ± 0.13	1.13 ± 0.05	1.21 ± 0.04	ns
Day 0 -76	1.01 ± 0.02	Day 0 -68	1.02 ± 0.07	1.03 ± 0.02	1.02 ± 0.04	ns

3.3 Benchmark dose model

Dose-response data was retrieved by using the benchmark dose model provided by EFSA. The benchmark dose limit (BMDL) is the lowest dose where treatment has an no effect. For Bea, the BMDL was estimated to be 321 µg/kg and 511µg/kg for the SGR and K-factor, respectively as seen in Table 7. The BMDL for EnnB was estimated to be 248 µg/kg and 259 µg/kg for SGR and SLR, respectively, as seen in Table 7. The low ratios indicate a precise confidence interval. Further analyses on tissue pathology, digestibility, organ function, blood parameters, oxidative stress, bone formation and other parameters are still in progress.

Table 7. Benchmark dose level (BMDL) analysis based on summary data of all subgroups where treatment had a significant effect; time period mid to end of trial (0-76 days for beauvericin and 0-68 days for enniatin B). 90% confidence interval.

	Beauvericin			Enniatin B	
	BMDL (µg/kg)	Ratio		BMDL (µg/kg)	Ratio
Specific growth rate:	321	14.4	Specific growth rate:	248	4.23
Condition factor:	511	4.29	Specific length rate:	259	4.25

3.4 Ex Vivo intestinal leakage

During dissection some of the intestines were damaged. These technical outliers were excluded from the dataset. The apparent permeability of intestines from different feeding groups is presented in Figure 9 and Figure 10. Significance was tested by Kruskal-Wallis test followed by Dunnet's multiple comparison test.

The distal intestinal segments of Atlantic salmon exposed from start to end of trial (0-68 days) to low, medium, and high dose EnnB (0.25 mg/kg, 5 mg/kg and 80 mg/kg, respectively) exhibit no evident trends, as seen in Figure 9. All the groups in figure 9 are overlapping, and ENN1 and ENN3 display a high variation. There was a non-significant difference among means compared to the control, $p > 0.05$.

Figure 10 presents the apparent permeability of distal intestinal sacs of Atlantic salmon in the control group and low, medium, and high dose Bea exposure (0.25 mg/kg, 5 mg/kg, and 25 mg/kg, respectively). The control group is within a lower range than the exposed groups. The median is increasing from BEA1, BEA2 to BEA3 indicating a dose-dependent increase in permeability. In which BEA1 and BEA3 treatment had a significant effect on the permeability compared to control, $p < 0.05$. BEA3 exhibits high variation.

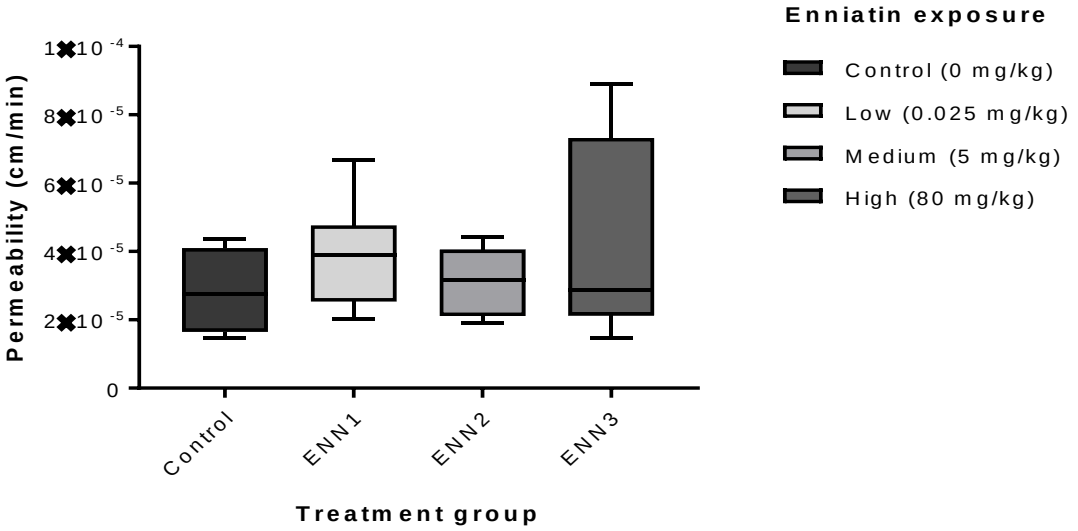

Figure 9. Apparent permeability (cm/s) of Atlantic salmon distal intestinal sacs *(Salmo salar)* from four different treatment groups of enniatinB exposure. The control group represents individuals given feed containing 0 mg/kg enniatin. ENN1, ENN2 and ENN3 representing diet groups containing low- (0.25 mg/kg), medium- (5 mg/kg) and high dose (80 mg/kg) enniatin, respectively. n = 6. Data is presented as mean ± SD. Apparent permeability was calculated as explained in methods, 2.6 Ex vivo intestinal leakage .

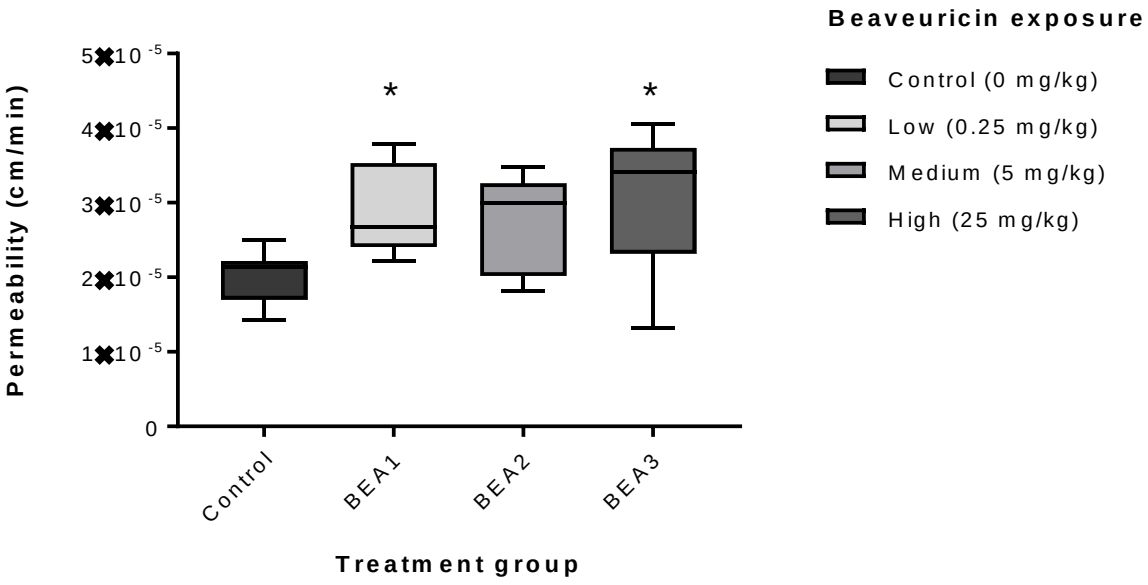

Figure 10. Apparent permeability (cm/s) of Atlantic salmon distal intestinal sacs *(Salmo salar)* from four different treatment groups of beauvericin exposure. The control group represents individuals fed on feed containing 0 mg/kg beauvericin. BEA1, BEA2, and BEA3 represents diet groups containing low- (0.25 mg/kg), medium- (5 mg/kg), and high dose (25 mg/kg) of beauvericin, respectively. n = 6. Data is presented as mean ± SD. Apparent permeability was calculated as explained in methods, 2.6 Ex vivo intestinal leakage . *$p < 0.05$

3.5 Histology

Histological results from control group, high dose enniatin (ENN3) and high dose beauvericin (BEA3) exposed groups are presented respectively in Figure 12, Figure 13 and Figure 14. High dose EnnB refers to a concentration of 80 mg/kg and high dose Bea refers to a concentration of 25 mg/kg. The distal intestinal segments of Atlantic salmon were cut in half, with the intention of fully exposing the intestinal lumen as presented in Figure 11.A. Half of the samples were cut in-half post fixation in 7% formaldehyde, which caused no contraction of the circular muscle tissue thereby no exposure of intestinal lumen as presented in Figure 11.B. The intestinal segments from all groups displayed a normal morphological appearance, with no significant shortage of intestinal folds (Figure 15). Morphological structures observed in the histological results were lamina propria, muscularis externa, submucosa, muscularis mucosae, blood vessels and enterocytes. There was no detection of increased infiltration of immune cells in exposed fish and thereby no observed enlargement of lamina propria. Goblet cells were regularly distributed in all groups, but with variation between individual fish. All groups displayed an intact brush border at the luminal surface of the enterocytes. Technical artifacts like squeeze, tissue tear- and orientation artifacts were observed in all groups (figure 14).

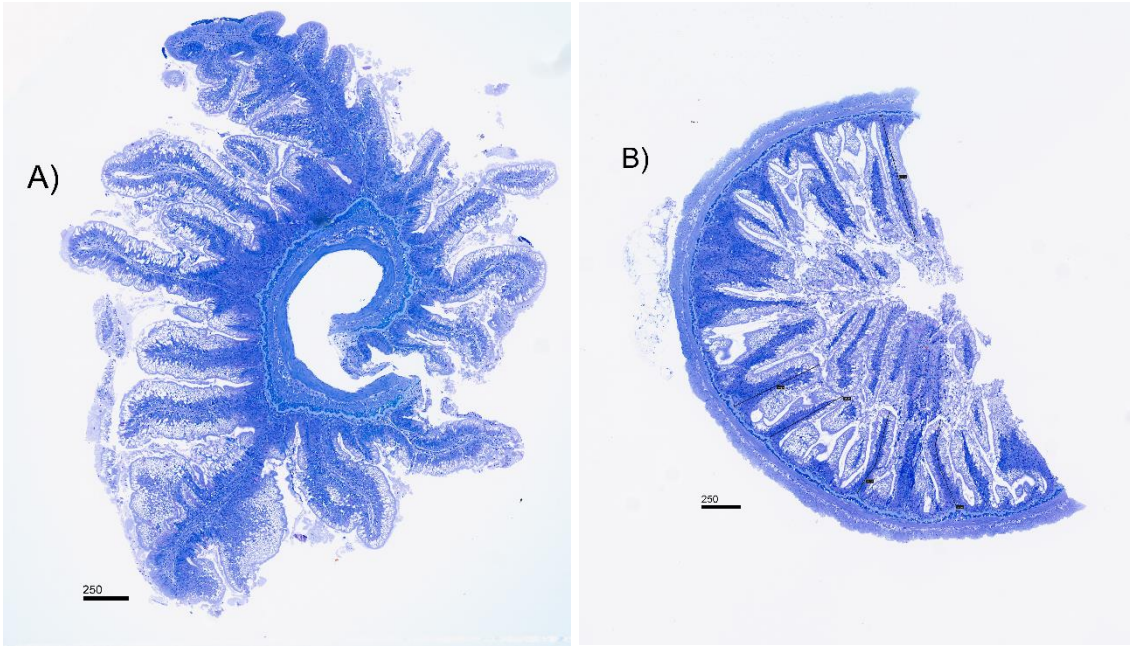

Figure 11. An overview of the orientation of embedded distal intestinal segments of Atlantic salmon *(Salmo salar).* A) fully exposing the intestinal lumen with the folds facing outwards, B) Half-moon shaped, not fully exposing the intestinal lumen and folds facing inwards.

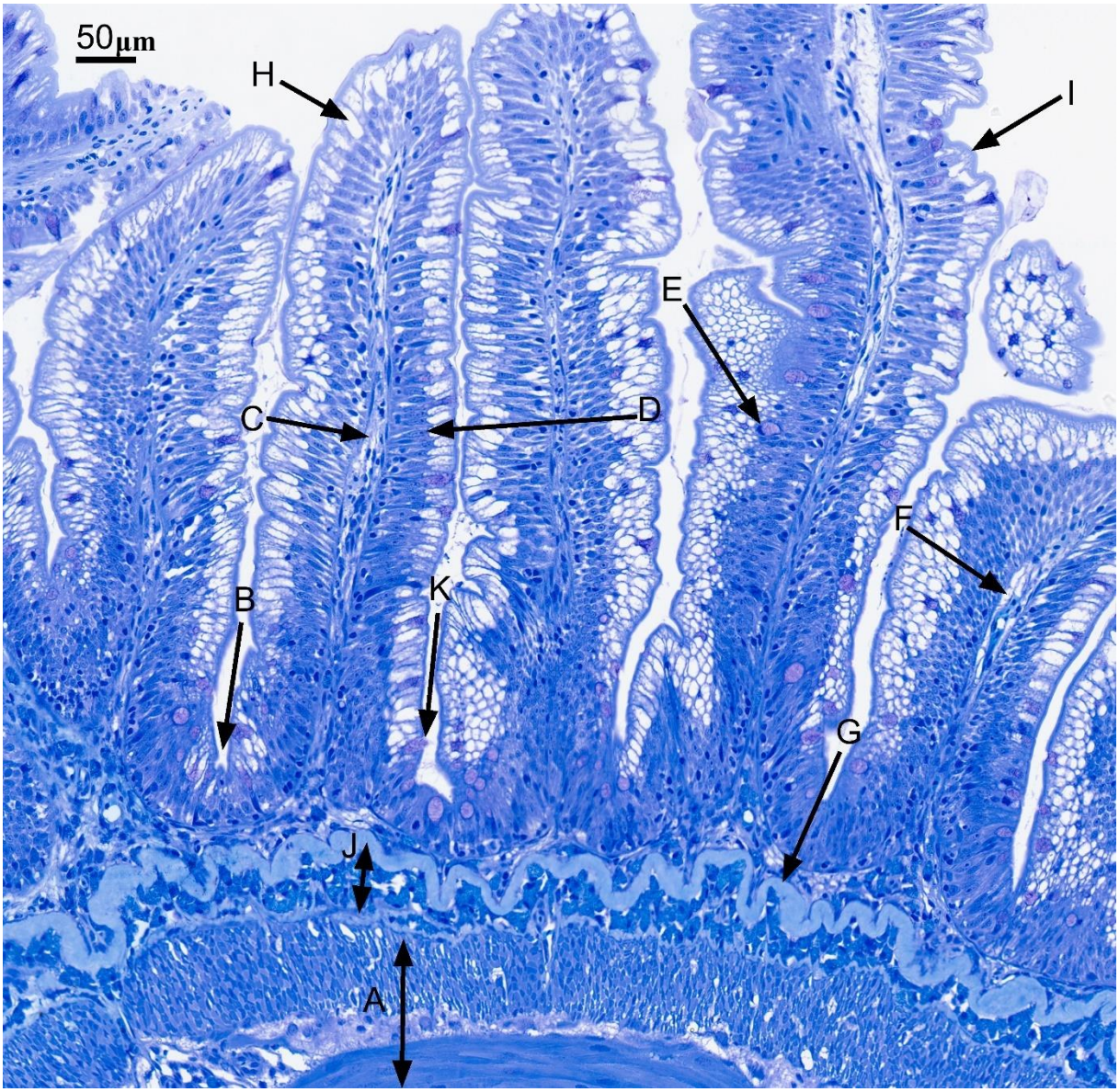

Figure 12. Histological appearance of a transverse cross section of distal intestinal tissue in Atlantic salmon *(Salmo Salar)* from the control group. The control group represents individuals fed on feed containing 0 mg/kg beauvericin and 0 mg/kg enniatin. The intestinal cuts were stained by toluidine blue and images digitalized by using NanoZoomer® S60, software NDP®.view2 and ImageJ. A - Muscularis externa, B – Crypt, C – Lamina propria, D – Nuclei, E – Goblet cell, F- Blood vessel, G – Muscularis Mucosae, H – Lipid droplet, I – Brush boarder, J – Submucosa , K – Secretion of mucus from goblet cell

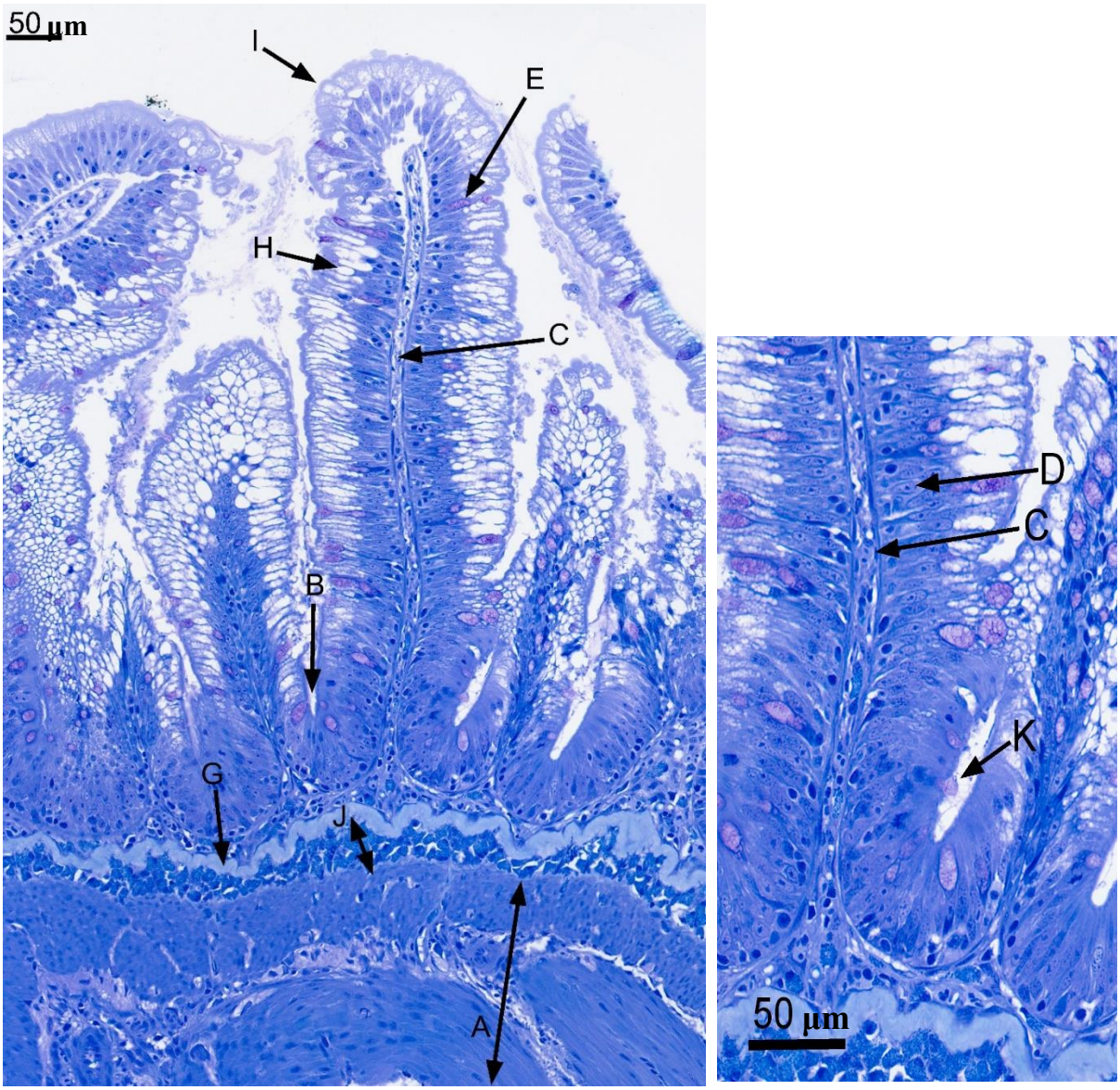

Figure 13. Histological appearance of a transverse cross section of distal intestinal tissue in Atlantic salmon *(Salmo Salar)* from the high dose enniatin exposed group, which represent individuals fed on feed containing 80 mg/kg enniatin. The intestinal cuts were stained by toluidine blue and images digitalized by using NanoZoomer® S60 , software NDP®.view2 and ImageJ. A - Muscularis externa, B – Crypt, C – Lamina propria, D – Nuclei, E – Goblet cell, G – Muscularis Mucosae, H – Lipid droplet, I – Brush boarder, J – Submucosa, K – Secretion of mucus from goblet cell

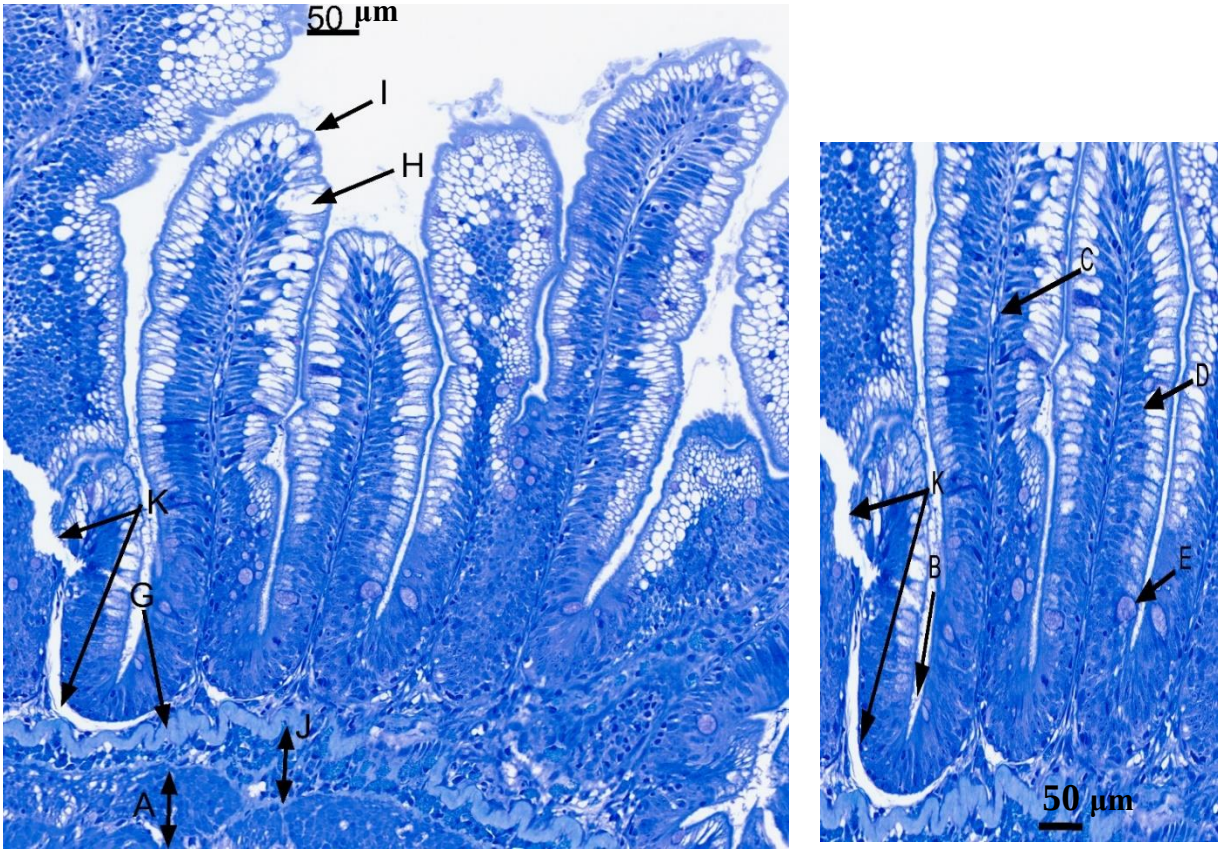

Figure 14. Histological appearance of a transverse cross section of distal intestinal tissue in Atlantic salmon *(Salmo Salar)* from the high dose beauvericin exposed group, which represent individuals fed on feed containing 25 mg/kg beauvericin. The intestinal cuts were stained by toluidine blue and images digitalized by using NanoZoomer® S60 , software NDP®.view2 and ImageJ. A - Muscularis externa, B – Crypt, C – Lamina propria, D – Nuclei, E – Goblet cell, G – Muscularis Mucosae, H – Lipid droplet, I – Brush boarder, J – Submucosa, K – Tissue-tear artifact.

The length of the distal intestinal folds is presented in Figure 15. The measurement in the three groups showed no significant differences and variation was high. The control group ranged from 500 to 1400 µm in length and ENN was within the same interval. BEA displayed a slightly lower measurement-interval.

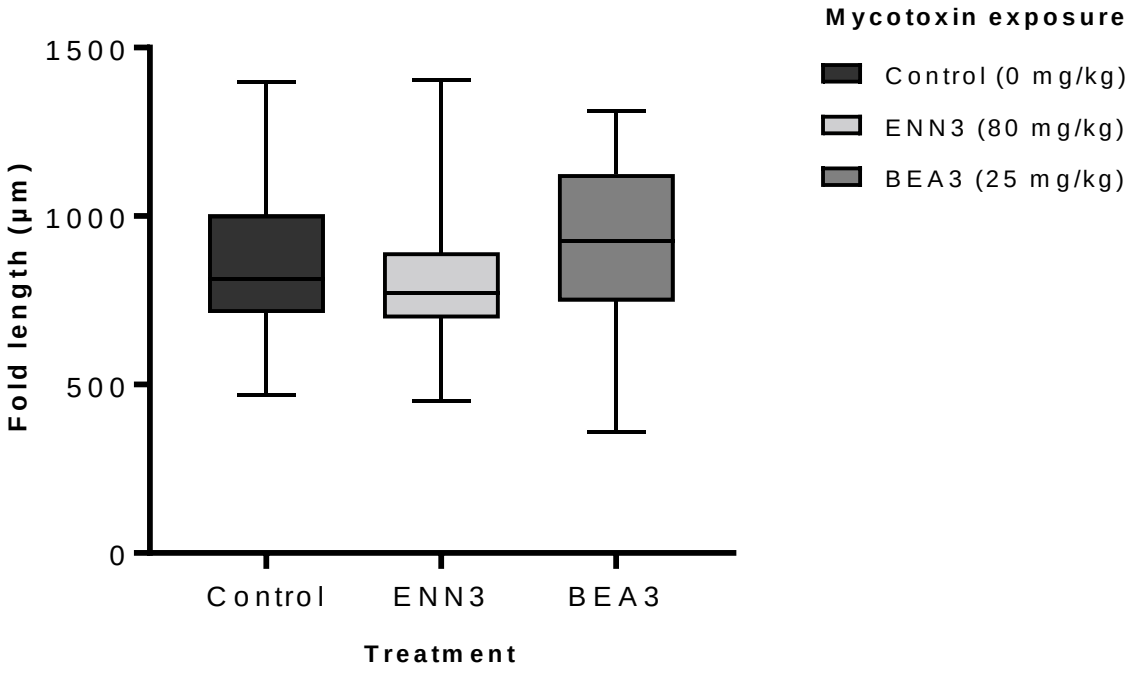

Figure 15. Measured fold length (µm) of the two longest folds from each Atlantic salmon *(Salmo salar)* distal intestinal segment from three different treatment groups. n=6. The control group represents individuals fed on feed containing 0 mg/kg beauvericin and 0 mg/kg enniatin. ENN3 represent high dose exposure of enniatin (80 mg/kg) and BEA3 represent high dose exposure beauvericin (25 mg/kg). Data is presented as mean ± SD.

3.6 Gene Expression

3.6.1. One step RT-PCR

Potentially relevant primers were tested using QUIAGEN OneStep RT-PCR kit and agarose (1%) gel electrophoresis in advance of the qPCR reaction. Intense bands at correct size were observed for most of the primers. Exceptions were *Hprt* D), *SOCS1_1* (E), *SOCS2*_2 (F) and *PCNA* (K) which displayed several weak bonds and were therefore excluded from further analysis (Appendix C, figure C1)

When testing the selected primers on a dilution series, numerous primers showed optimal Cq values < 29.0 in addition to a single peak melting curve. The *Sema3a* primer exhibited a Cq value close to 29.0 (28.9) plus multiple melting curve peaks. Additionally, IL6B displayed a Cq value > 29.0. This was interpreted as factors of low level of specificity and representing multiple amplicons and was therefore consequently left out.

3.6.2 Transcription of genes

The qPCR results for all genes and groups were significantly tested by Kruskal-Wallis One-Way ANOVA followed by Dunnetts multiple comparisons post hoc test. There was not observed a clear dose-dependent increase in any of the gene expressions. The genes where treatment group had a significant effect on the expression were *MnSOD* (ENN1), *SOCS2* (ENN3), *Gpx4* and *ALAS1* (BEA1). The control for enniatin- and beauvericin exposures is individual, due to sampling-date variation between the two groups.

The transcription of genes related to oxidative stress is presented in Figure 16. The enniatin exposed treatment groups had a non-significant effect on the *Gpx4* expression compared to the control (Figure 16, A). The *Gpx4* expression in BEA1, BEA2 and BEA3 had higher mean expression compared to the control, but BEA1 was the only treatment that had a significant effect, $p < 0.05$ (Figure 16, B). For the *GPx3*-gene, none of the treatment groups had a significant effect (Figure 16, C and D). The expression of *GPx3* in enniatin exposed groups showed high individual variation (Figure 16, C). For the beauvericin exposed groups, *GPx3* display the same non-significant expression pattern as the enniatin-exposed ones, although BEA1 being the only treatment with high variation (Figure 16, D).

The expression level of *MnSOD* exhibited a similar trend in all treatment groups for both enniatin and beauvericin exposure (Figure 16, E and F). For enniatin, the expression level in the control was lower than all exposed groups (Figure 16, E). *MnSOD* was only significantly upregulated in ENN1 compared to control, $p < 0.05$. The mRNA expression of *MnSOD* in the beauvericin exposed groups were all non-significant compared to the control (Figure 16, F).

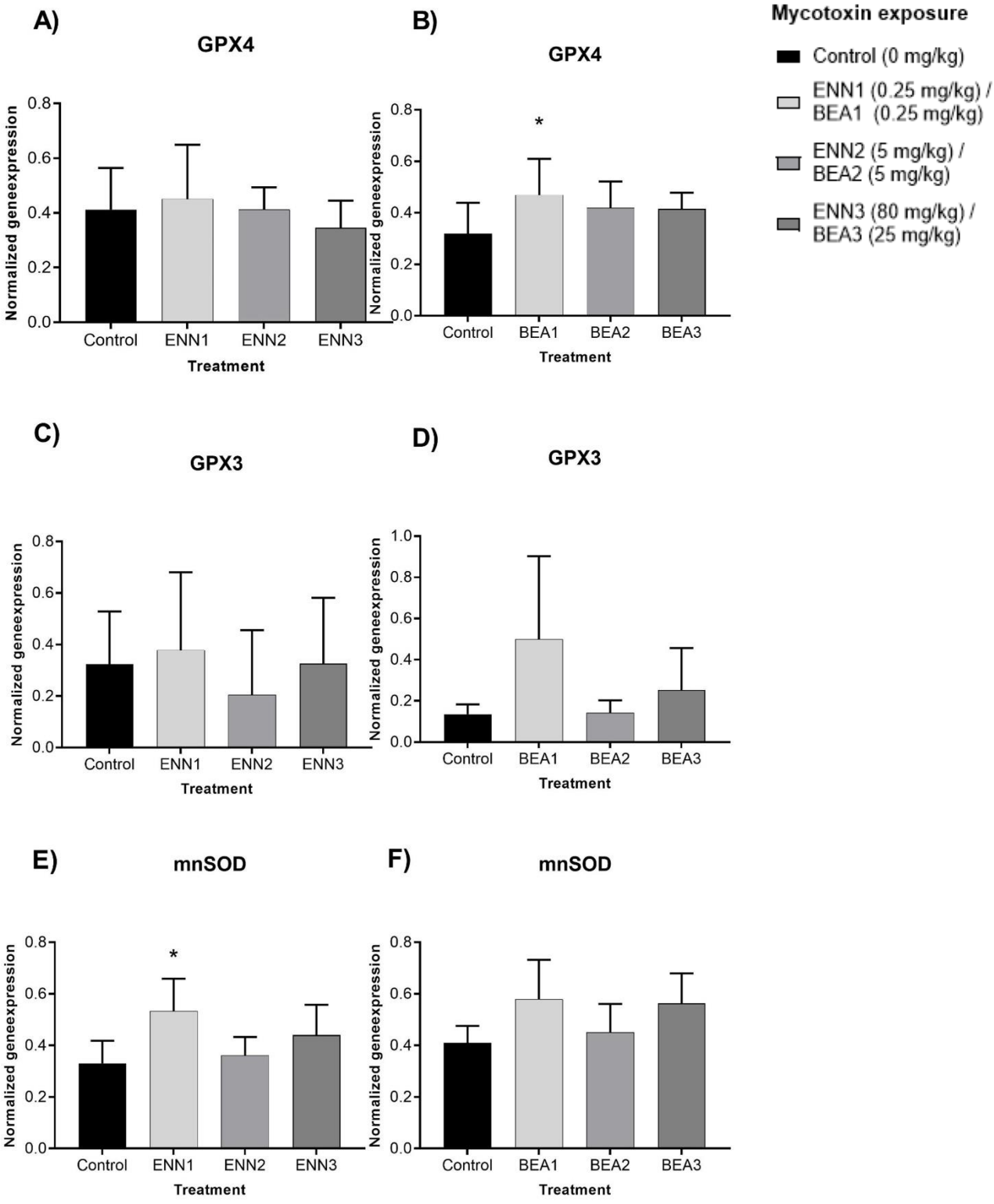

Figure 16. The mRNA expression of genes in Atlantic salmon *(Salmo salar)* related to oxidative stress in seven different treatment groups, n = 6. *Gpx4* expression in individuals exposed to low*, medium and high dose enniatin (A) and beauvericin (B), *GPx3* expression in individuals exposed to low, medium and high dose enniatin (C) and beauvericin (D) and *MnSOD* expression in individuals exposed to low, medium and high dose enniatin (E) and beauvericin (F). ENN1, ENN2 and ENN3 corresponds to low, medium and high dose exposure enniatin (0.25 mg/kg, 5 mg/kg, 80 mg/kg, respectively). BEA1, BEA2 and BEA3 corresponds to low, medium and high dose exposure beauvericin (0.25 mg/kg, 5 mg/kg and 25 mg/kg, respectively). Data is presented as mean ± SD. *$p < 0.05$

5.5.3 Transcription of genes related to intestinal structure and function

There was no treatment group that had a significant effect on the expression level of GADD45 or PCNA, compared to control. The highest mRNA expression of GADD45 amongst enniatin treatment groups and control was ENN2, although the variation was also higher in ENN2 compared to the other groups and control as seen in Figure 17, A. The control, ENN1 and ENN3 was approximately the same gene expression level. For the GADD45 gene in beauvericin exposed groups, a peak was observed in BEA1 compared to control as seen in Figure 17, B.

PCNA expression in enniatin treatment groups displayed a peak in ENN1 in comparison to the control, presented in Figure 17, C. While ENN2 and ENN3 displayed decreasing trend. Whereas the beauvericin exposed exhibited the highest expression level of PCNA in the control group as shown in Figure 17, D. BEA1 slightly lower than both BEA2 and BEA 3, which was at the same expression level.

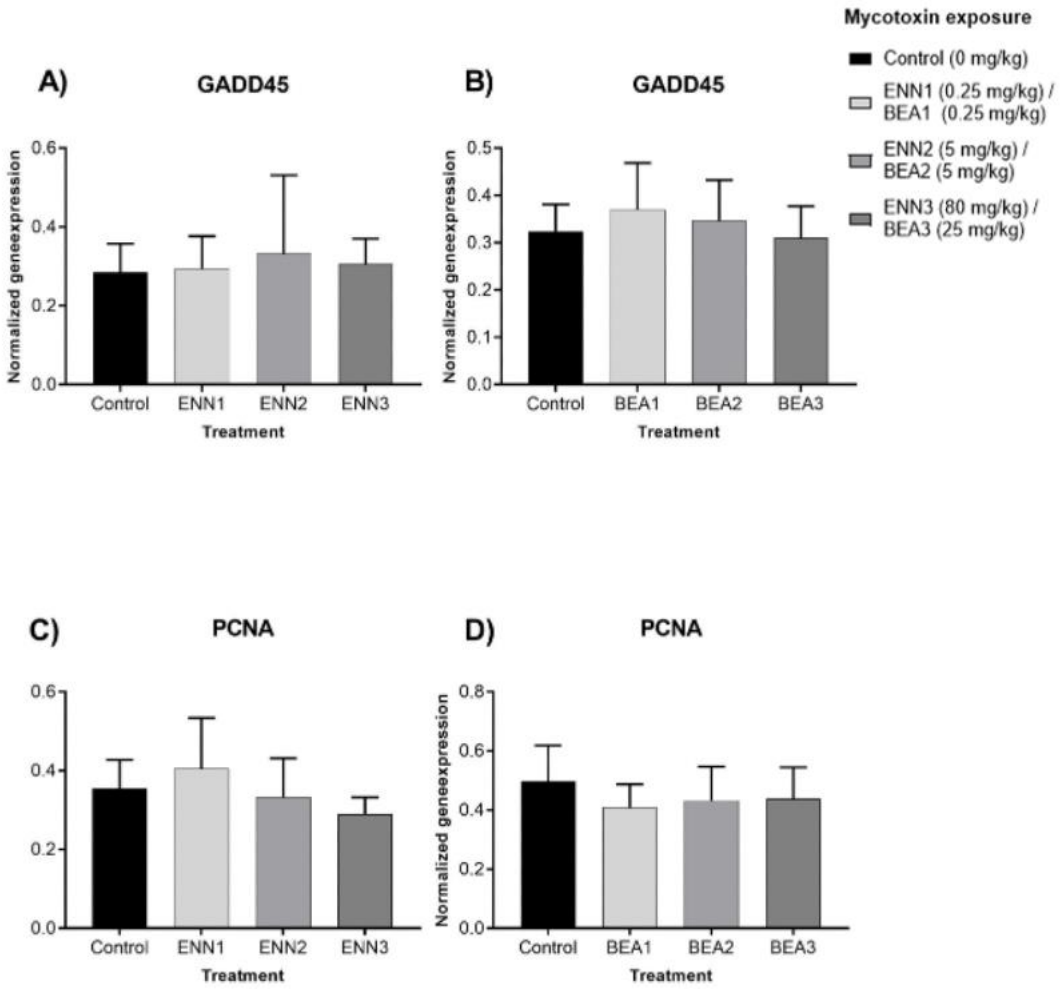

Figure 17. The mRNA expression of genes in the distal intestine of Atlantic salmon *(Salmo salar)* related to intestinal structure and function in seven different treatment groups, n = 6. *GADD45* expression in individuals exposed to low, medium and high dose enniatin (A) and beauvericin (B) and *PCNA* expression in individuals exposed to low, medium and high dose enniatin (C) and beauvericin (D). ENN1, ENN2 and ENN3 corresponds to low, medium and high dose exposure enniatin (0.25 mg/kg, 5 mg/kg, 80 mg/kg, respectively). BEA1, BEA2 and BEA3 corresponds to low, medium and high dose exposure beauvericin (0.25 mg/kg, 5 mg/kg and 25 mg/kg, respectively). Data is presented as mean ± SD.

There was no treatment group that had a significant effect on the expression level of *occludin* or *CLDN25b*, compared to control. For enniatin, all treatment groups showed higher expression level of *occludin* control, illustrated by Figure 18, A. ENN3 resulted in the highest expression, while ENN2 had the lowest gene expression. ENN1 was in between ENN2 and ENN3. However, for the beauvericin exposed groups, BEA1 exhibited the highest expression level of *occludin* (Figure 18, B). The *occludin* expression in BEA2 and BEA3 was higher than control, although lower than BEA1.

For the expression of *CLDN25b* amongst enniatin exposure, ENN1 displayed the highest expression compared to the control (Figure 18, C). ENN2 was slightly upregulated compared to the control, while ENN3 was downregulated. Beauvericin exposure resulted in a different pattern of *CLDN25b* expression (Figure 18, D). BEA3 and BEA1 was higher compared to control, and BEA2 was lower.

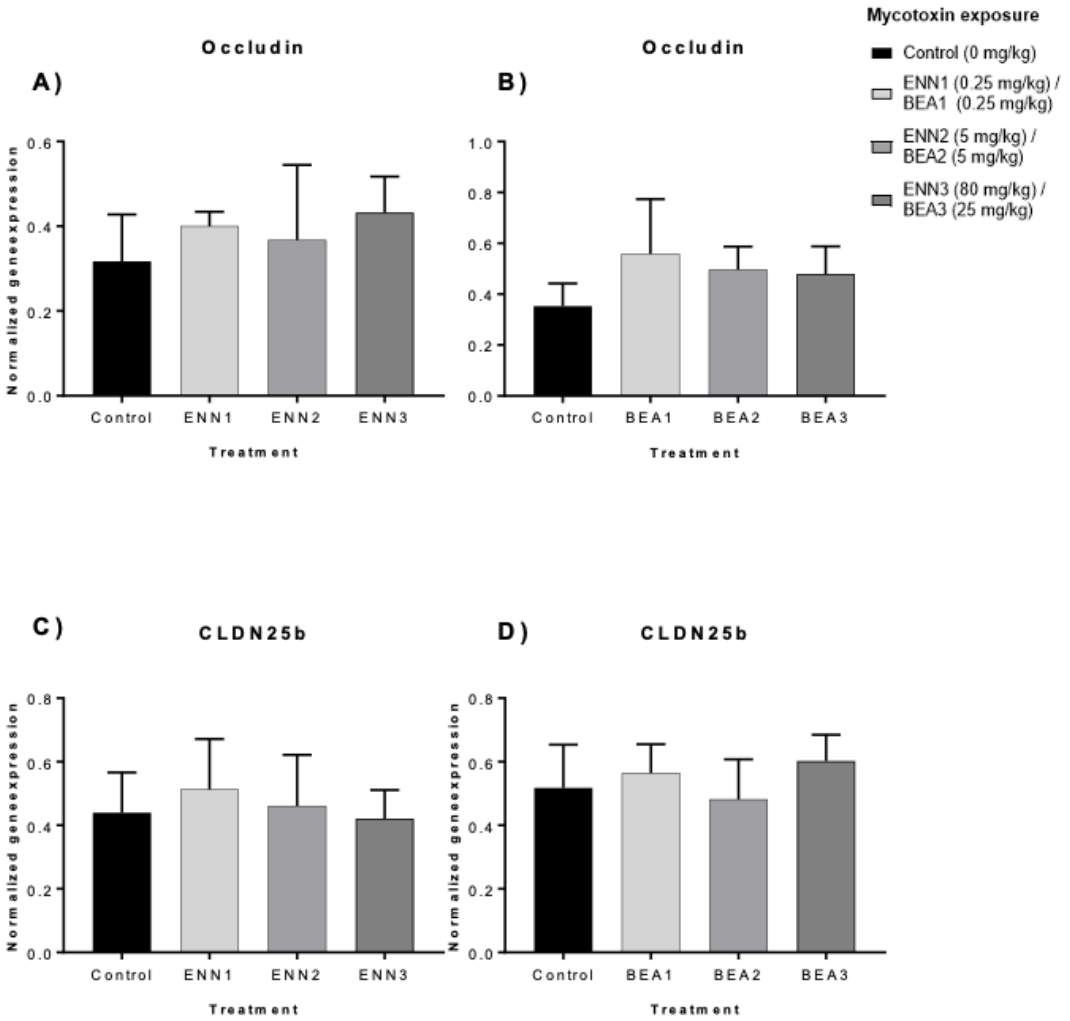

Figure 18. The mRNA expression of genes in the distal intestine of Atlantic salmon (*Salmo salar)* related to intestinal structure and function in seven different treatment groups, n = 6. *OCLN* expression in individuals exposed to low, medium and high dose enniatin (A) and beauvericin (B) and *CLDN25b* expression in individuals exposed to low, medium and high dose enniatin (C) and beauvericin (D). ENN1, ENN2 and ENN3 corresponds to low, medium and high dose exposure enniatin (0.25 mg/kg, 5 mg/kg, 80 mg/kg, respectively). BEA1, BEA2 and BEA3 corresponds to low, medium and high dose exposure beauvericin (0.25 mg/kg, 5 mg/kg and 25 mg/kg, respectively). Data is presented as mean ± SD.

The expression of *SOCS2* in the distal intestine of Atlantic salmon was significantly increased in ENN3 compared to control, $p < 0.05$ (Figure 19, A). ENN2 and ENN1 had expression levels higher than control although non-significant. had the highest expression of *SOCS2* amongst enniatin exposed groups, although non-significant. None of the beauvericin exposed

treatment groups had a significant effect on expression levels of *SOCS2* compared to the control (Figure 19, B). BEA1, BEA2 and BEA3 displayed a decreasing trend.

The expression of *ALAS1* in enniatin exposed groups was non-significant. *ALAS1* displayed the highest expression in ENN1 amongst the enniatin exposed groups, compared to the control (Figure 19,C). For the beauvericin exposed groups, BEA1 had a significant effect on the gene expression of *ALAS1* compared to the control, $p < 0.05$ (Figure 19, D). BEA2 and BEA3 displayed a decreasing trend, although higher expression compared to the control and non-significant.

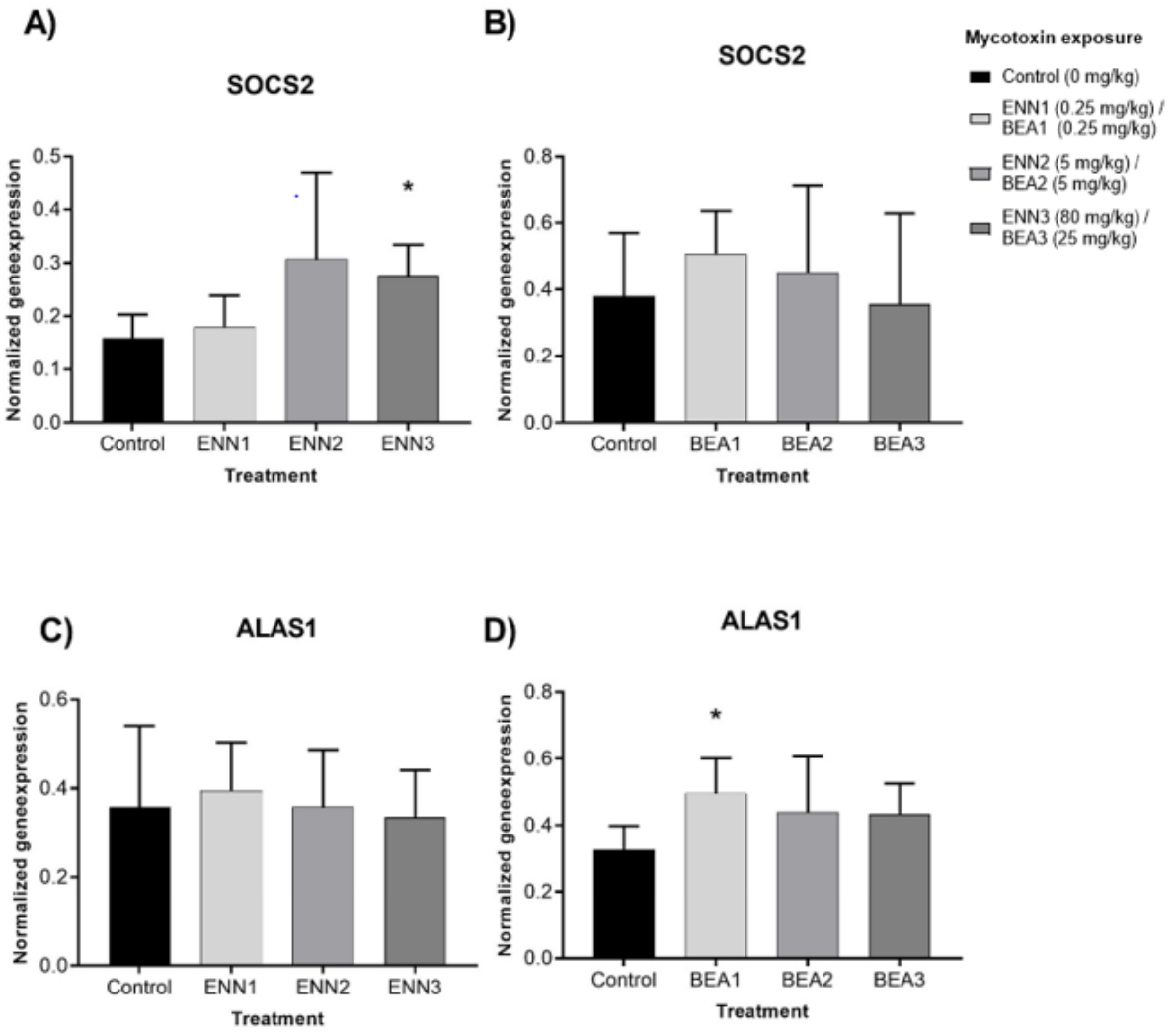

Figure 19. The mRNA expression of genes in distal intestine of Atlantic salmon (*Salmo salar)* related to cytokine signaling (*SOCS2*) and heme biosynthesis (*ALAS1*) in seven different treatment groups. n = 6. *SOCS2* expression in individuals exposed to low, medium and high dose* enniatin (A) and beauvericin (B) and *ALAS1* expression in individuals exposed to low, medium and high* dose enniatin (C) and beauvericin (D). ENN1, ENN2 and ENN3 corresponds to low, medium and high dose exposure enniatin (0.25 mg/kg, 5 mg/kg, 80 mg/kg, respectively). BEA1, BEA2 and BEA3 corresponds to low, medium and high dose exposure beauvericin (0.25 mg/kg, 5 mg/kg and 25 mg/kg, respectively). Data is presented as mean ± SD. *$p < 0.05$

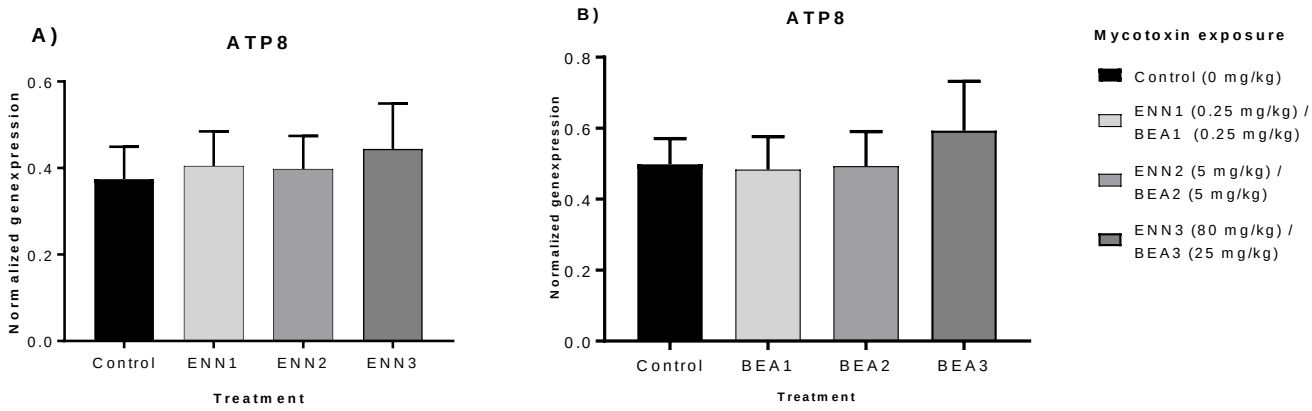

Figure 20. The mRNA expression of ATP8 in distal intestine Atlantic salmon (*Salmo salar*) seven different treatment groups. n = 6. ATP8 expression in individuals exposed to low, medium and high dose enniatin (A) and beauvericin (B). ENN1, ENN2 and ENN3 corresponds to low, medium and high dose exposure enniatin (0.25 mg/kg, 5 mg/kg, 80 mg/kg, respectively). BEA1, BEA2 and BEA3 corresponds to low, medium and high dose exposure beauvericin (0.25 mg/kg, 5 mg/kg and 25 mg/kg, respectively). Data is presented as mean ± SD.

4. Discussion

The aim of this thesis was to investigate if long term exposure of two mycotoxins, enniatin B and beauvericin, had any adverse effect on the intestinal health of Atlantic salmon (*Salmo salar*). A three-month exposure trial was conducted at Matre, where fish was divided into seven different treatment groups. Control-, low-, medium- and high dose exposure of enniatin B or beauvericin. After finished trial, the toxicity of each compound was evaluated though an intestinal permeability assay, histological evaluation and expression of genes related to intestinal function and xenobiotic stress.

4.1 Does EnnB and Bea cause impaired growth in salmon?

As an indicator of impaired aquacultural preformance of Enniatin B (EnnB) and Beauvericin (Bea) exposure, impaired growth was observed in both treatment groups. The Bea exposed fish got thinner, but also displayed an increased feed intake in the period 32-76 days of exposure. Despite this increased feed intake in Bea exposed fish, a dose-dependent reduction of CF was also observed along with a higher FCR. Previous research has shown that salmonids try to compensate for poor utilization of feed through increasing the intake of feed (Kaushik and Médale, 1994). This could be reflected through the dose – dependent increase of FCR in Bea treatment groups, indicating reduced feed utilization. Hence, an imbalance in metabolism could be plausible to assume. Which was suggested by Søderstrøm et al. (2022), in Atlantic salmon hepatocytes where an increased energy expenditure and elevated oxidative stress was demonstrated when exposed to Bea and EnnB, individually.

An impaired growth was also noticed following EnnB treatment, but in a different manner compared to Bea. The high dose EnnB exposure caused bone deformities at the end of trial and significantly reduced weight and length. As opposed to Bea exposed fish, the CF factor, feed intake and FCR were not significantly affected with increased dietary EnnB levels. Thus, one could assume that the reduced growth in EnnB treatments is a consequence of the observed bone deformities. Or conversely, bone deformities being a result of reduced growth. Alternatively, the bone deformities are due to effects on mineralization. This implies EnnB of having a direct effect on the skeletal structure, compared to the intestine. While the growth

impairments in Bea seems to be due diminishing ability to utilize feed, indicating a more direct effect on the intestine.

Although there is a lack of scientific data on the effect of beauvericin and enniatin exposure of fish, some mammalian in vivo studies have been conducted where impaired growth was shown. A 42 day sub-chronic exposure study (gavage feeding) on mice was performed, investigating the effects of EnnB and Bea (Maranghi et al., 2018). Similarly to our findings, the study showed a reduced weight in both male and female mice exposed to EnnB. Female mice had reduced weight in low (0.8 mg/kg BW) and high dose (19 mg/kg BW) while male mice had reduced weight in high dose only (18 mg/kg BW). The dosage by Maranghi et al. (2018) were notably based on mg/BW per day, while the doses in the present trial were set at mg/kg feed. This contributes to an uncertainly as the doses are not directly comparable. Nonetheless, the same trial resulted in an increased food intake, which was not observed for the EnnB treated salmon, but more in line with the effects of Bea in the present study.

The food intake in Bea exposure (1 mg/kg BW) of the EFSA study was significantly increased for male mice (Maranghi et al., 2018). Interestingly, the weight gain was not altered, in line with the present results on salmon. This could imply an impaired uptake of nutrients. In contrast, a subacute 9 day study reported no effect of injected Bea (5 mg/kg) or EnnB (5 mg/kg) on mice weight gain or food consumption (Rodríguez-Carrasco et al., 2016). Additionally, broiler chicks exposed to Bea for 37 days were not negatively affected in regards of weight gain or FCR (Leitgeb et al., 2003). The two latter studies contradict our study which showed that oral Bea exposure exerted negative effects on growth, utilization of feed while simultaneously leading to an increased feed consumption. Importantly, the degree of toxic response in general can vary depending on species, individual sensitivity, exposure route and dosage (Burcham, 2014). Ultimately making it challenging to provide an accurate comparison across species and studies.

4.2 Beauvericin increased the intestinal permeability

The *ex vivo* gut sac model (Figure 7) performed in the present study, has previously been proven well suited for an assessment of intestinal integrity (Mateer et al., 2016). To our knowledge, this kind of assay has not been previously performed on animals exposed to

mycotoxin. The distal intestinal segment was chosen as research suggests it to be important for immunological defense and has also been shown to be prone to inflammatory disorders in salmon (Moldal et al., 2018).

A well-functioning intestinal is essential to maintain an optimal health and growth, which presumably is impaired in Bea treated fish, indicated by the non-optimal feed utilization. The ionophoric capability of Bea to transport cations, Ca^{2+} specifically, across biological membranes can disturb the intracellular homeostasis further disrupting cell- and organelle function (Søderstrøm et al., 2022, Wu et al., 2018). This could moreover affect the paracellular tight junction (TJ) control, resulting in the increased intestinal permeability. A suboptimal control of paracellular permeability could then result in leakage of macromolecules such as food particles (Gao et al., 2020). A secondary consequence of the leakage might be inflammation or reduced growth, as observed from the dose-dependent reduction of both SGR and CF and in Bea treatment groups. Whereas the upregulated expression of both *Gpx4* and *ALAS1* in Bea exposed groups could also be indicating an effect of Bea exposure. An increased Gpx activity due to Bea exposure has also been seen *in vitro* Atlantic salmon cell line, where a high cytotoxic potential of these contaminants was established, further strengthening this explanation (Søderstrøm et al., 2022).

Furthermore, given that early signs of smoltification were observed at the end of trial, one could assume altered permeability due to preparation of increased drinking rates and ion- and fluid transport in the intestine (McCormick, 2012). However, a study on TJ expression in intestinal tract of Atlantic salmon showed no alteration of genes before actual entering of the saltwater phase (Tipsmark et al., 2010). One could also speculate that Bea's ability to be incorporated into the lipid bilayers and act as an ionophore is related to the observed increased permeability in this trial.

Increased intestinal permeability in Atlantic salmon has been reported as an effect of saponin exposure (Knudsen et al., 2008). Enteritis in the distal intestine was also observed in connection with increased permeability. However, Knudsen et al. (2008) specifies that the

observed inflammation is a secondary effect of the increased permeability, due to infiltration of bacteria's disrupting the gut microbiota.

Similar to Bea, EnnB also possesses a lipophilic structure (Krug et al., 2018). Providing the ability to incorporate into biological membranes where it can function as an ionophore, facilitating transport of cations across the lipid bilayer, disrupting the homeostasis in the intracellular environment. Despite this similar structure, none of the EnnB treatment groups had a significant effect on the apparent permeability. Which is in line with no effect in PCNA or GADD45, indicating no increased cell proliferation or regulation of proteins related to growth and apoptosis. A study conducting this same *ex vivo* permeability method on broiler chickens also showed no effect of mycotoxin exposure, notably with *AflatoxinB_1* (Galarza-Seeber et al., 2016). Nevertheless, chickens may have evolutionary adapted to many kinds of mycotoxins, being a terrestrial animal where ingestion of mycotoxins are common and have been for a long time.

However, there was also observed a higher variation in all EnnB groups in the permeability measurements in comparison to Bea, possibly indicating uncertain measurements. When performing an ex vivo model as presented in this study, it is crucial that physiological parameters are optimal to provide reliable results. The regional consistency is also important when conducting this kind of assay (Mateer et al., 2016). The distal intestine was the selected region, although the size, i.e. length, of the segments varied. Additionally, the amount of FITC-D injected into the segments, were on sampling-site determined to be 1 µl per gram of bodyweight (BW) per individual to set a standardized amount. In retrospect it would be more suitable to adjust the injected volume according to the size dissected intestinal segment, rather than BW. This could have caused under- or overdistention of the segments, which might have led to inconsistency between samples (Mateer et al., 2016). This could be an explanation to the high variation observed in the apparent permeability in the EnnB treatment groups.

The inconsistency in effects of Bea and EnnB in the present study could also be caused by different metabolization of the two compounds. A study by Rodrígues-Carrasco et al. (2016) suggested a higher chronic toxicity of Bea in mice, compared to EnnB. An assumption based on higher detection of Bea in fat rich tissue, thus indicating a lower bioavailability of EnnB. Furthermore indicating Bea of entering the enterohepatic recycling thus being able to elicit more damage to the intestine, while EnnB being rapidly metabolized (Rodríguez-Carrasco et al., 2016). This is in line with and strengthen the results acquired from the permeability measurements.

4.3 Increased permeability not reflected by the histological assessments

Despite impaired growth in both groups in addition to increased permeability in Bea treatments, no histological abnormalities were observed in the distal intestine of Atlantic salmon. Mycotoxin-induced enteritis in Atlantic salmon has not been described through histological evaluations yet, however enteritis caused by saponins is well documented. Inflammatory indicators of the distal intestine of Atlantic salmon include edema of lamina propria, increased infiltration of immune cells, loss of supranuclear vacuoles and reduced mucosal height (Knudsen et al., 2007). The histological assessments in high dose EnnB (80mg/kg) and high dose Bea (25 mg/kg) displayed no morphological indicators of enteritis, based on the intestinal fold-length measurements and overall impression. In a study done on weaning piglets, no significant effects of deoxynivalenol (DON) or EnnB + Bea were seen in the morphology of intestinal tissue, although disrupted intestinal integrity was observed (Novak et al., 2021). However, reduced mucosal fold height has been observed in animals exposed to mycotoxins; in broiler chickens following Aflatoxin exposure, in pigs following DON exposure, in turkeys and mice due to trichothecene exposure (Gao et al., 2020).

Even though the intestine, especially the distal part has a rather homogenous structure, it is an organ with a lot of activity. This is due to its dynamic barrier function which can result in high variation in measurements (Gao et al., 2020). The high variation displayed in all treatment groups of this trial, reflects the uncertainties in the histology measurements. The fact that no groups were starved pre- sampling gives a momentary picture of the intestine, but at the same time contributes to more variation. This was reflected by the abundance of lipid droplets (LD) present in the histology images in all treatment groups. If the individuals were put through

fasting pre-sapling, the lipids stored in the LD would have been assembled into lipoproteins like chylomicrons and transported thought the body (Ko et al., 2020). Which most likely would have reduced the individual variation. Unfortunately, artifacts were observed in all groups due to challenges during the tissue-embedding process resulting in improper orientation. This is essential when quantifying length measurements of villi. In addition these kind of measurement are not as objective as other methods (Rašković et al., 2011).

One could also speculate if the permeability assay would be a more sensitive endpoint compared to histology when evaluating disruption of intestinal integrity. As a suboptimal control of paracellular permeability would be a disruption of epithelial cells not visible through histology images to the naked eye.

Bea and EnnB have also been reported to alter the microbiota of the gut, which can also disrupt intestinal permeability (Novak et al., 2021); Bischoff et al., 2014). Perhaps a prolonged experimental period would provide visible effects through histological assessments, hence categorizing the increased permeability in the present trial as a first indicator of the effect of treatment.

The underlying toxicological mechanisms of EnnB and Bea are not fully known. Orally ingested mycotoxins are generally thought to induce harmful effect on the intestine. Effects like thinned mucus layer, disruption of epithelial cells and tight junctions, causing increased permeability (Gao et al., 2020) Hence, a regulation of tight junctions would be plausible to presume based on the observed increased permeability in low and high dose Bea. An *in vivo* study investigating the effect of DON in Atlantic salmon reported decreased biomarkers for tight junctions (*occludin*, *CLDN25b* and *tricellulin*) (Moldal et al., 2018). Suggesting an increased intestinal permeability, which was also observed in the present trial. However, no effect was seen in expression of either *CLDN25b* or *occludin* in the present trial. Interestingly, no observations of intestinal disruption were made by Moldal et al. (2018) following histological examination of the distal intestine, furthermore in line with our findings.

Additionally, Moldal et al., (2018) reported an increased *SOCS2* expression in the distal intestine of Atlantic salmon exposed to DON, just above guidance value (5.5 mg/kg feed).

Similarly, an upregulation of *SOCS2* was in high dose EnnB (80 mg/kg) in the present trial. SOCS proteins are suppressors of cytokine signalling involved in the control of inflammatory responses and can also control growth hormones through negative feedback (Skjestol et al.,2014). Therefore, as suggested by Moldal et al. (2018), these alterations this could be due to a more subtle mechanism of action.

4.4 Presumably sufficient energy turnover in the mitochondria

Several studies report an effect of EnnB and Bea on oxidative phosphorylation (Søderstrøm et al., 2022, Tonshin et al., 2010). Oxidative phosphorylation is a metabolic component of the energy turnover in the mitochondrion (Campbell et al., 2018). In which functional mitochondrial proteins is crucial for sufficient energy production (Campbell et al., 2018). According to the Comparative Toxicogenomics Database (CTD; http://ctdbase.org), ATP synthase membrane subunit 8 (*ATP8*) is a gene repeatedly occurring in *in vitro* studies in relation to enniatin and beauvericin exposure (Davis et al., 2020) (Appendix D, Figure D1 and D2). A study by Escriva et al. (2018) exposing EnnB and Bea to Jurkat-T cells showed an effect at a concentration of 1.5 µM on mitochondrial genes (including ATP8). Also, in co-exposure of EnnB + Bea, displayed a downregulation of mitochondrial genes even at concentration 0.5 µM (Escrivá et al., 2018). Likewise, ATP levels in hepatocytes of the *in vitro* trial by Søderstrøm et al. (2022) were affected by both EnnB and Bea, at concentrations of 5 µM. Whereas both trials supporting that the mechanism of toxicity for both EnnB and Bea is related to ionophoric properties. Interestingly the expression of *ATP8* in the present trial was not significantly affected by neither treatment groups.

Although *in vitro* studies are useful for describing an acute response and elucidate toxicological mechanisms, they do not provide the complex *in vivo* distribution and metabolism (Burcham, 2014). In which duration of exposure also is key. Underlined by the discrepancy between the *in vivo* and *in vitro* results of EnnB and Bea, regardless of dosage differences between methods. Furthermore, although the presumably sufficient energy turnover in mitochondria based on non-effect in *ATP8* expression, oxidative stress seemed to be induced by the treatment.

4.5 Oxidative stress as a consequence of ionophoric activity

As mentioned previously, oxidative stress is the proposed effect of many major mycotoxins (Da Silva et al., 2018). *MnSOD* (manganese superoxide dismutase) and *Gpx4* (glutathione peroxidase 4) are to two commonly used biomarkers for oxidative stress in Atlantic salmon (Olsvik et al., 2010). These two was upregulated in the present trial in low dose EnnB (0.25 mg/kg) and Bea (0.25 mg/kg), respectively. The functions of these two genes are however quite different. The *MnSOD* protein (encoding gene SOD2) is located in the mitochondria and functions by converting superoxide (oxidative stress byproduct) to less reactive hydrogen peroxide and oxygen. Accordingly, one could assume the upregulation of *MnSOD* in low dose EnnB (0.25 mg/kg) as a response to oxidative stress caused by mitochondrial reactive oxygen species (ROS). The mitochondrial ROS supposedly being caused by EnnB's ionophoric characteristics and negative effect on mitochondrial activity, as purposed by Søderstrøm et al. (2022).

Gpx4 on the other hand was not affected by low dose EnnB (0.25 mg/kg) treatment but upregulated in low dose Bea (0.25 mg/kg) in the present trial. The protein encoded by this *Gpx4* protect cells against membrane lipid peroxidation by converting free radicals intro harmless substances, like water (Xia et al., 2021). In an *in vitro* study by Søderstrøm et al. (2021), the activity of Gpx enzymes in hepatocytes was increased in a dose dependent manner due to Bea and EnnB exposure (individually). Similarly, lipid peroxidation has also been reported as an effect of Bea, but in combination with DON in Caco-2, cells displaying a synergistic effect (Kouadio et al., 2007). Possible synergistic effects of mycotoxins are not to be underestimated, as co-occurrence of mycotoxins frequently occur in nature (Jonsson, 2017). The upregulation of *Gpx4* in low dose Bea (0.025 mg/kg) could therefore be interpreted as a response to handle the ionophoric activities caused by Bea and protect the cells against membrane lipid peroxidation.

Further connecting the observations on presumed oxidative stress due to ionophoric activity of EnnB and Bea, an increase of ALAS1 was also observed in low dose Bea (0.025 mg/kg). *ALAS1* (5-aminolevulinate synthase) is a gene which is the first-rate limiting step through negative feedback in the mammalian heme biosynthetic pathway (Kubota et al., 2016). Heme is partially synthesized in the mitochondria and is essential to produce red blood cells and to

bind both oxygen and iron (Burcham, 2013). As an increase of *ALAS1* was observed our low dose Bea (0.025 mg/kg), it is plausible to assume a lack of heme due to the negative feedback mechanism. Heme deficiency could lead to iron dyshomeostasis, leading to oxidative stress. In Atlantic salmon hepatocytes exposed to EnnB and Bea individually, *ALAS1* was regulated (Søderstrøm et al., 2022). This was further connected to ferroptosis, where lipid peroxidation is one of the upstream mechanisms (Søderstrøm et al., 2022), in line with our findings of increased expression of Gpx4 in low dose Bea (0.025 mg/kg). Furthermore, blood parameters were also measured in the present trial (unpublished data) at mid-trial (day 32) where a decrease of hematocrit was observed in both low dose EnnB (0.25 mg/kg) and Bea (0.025 mg/kg). Connecting another link to the heme deficiency.

4.6 Benchmark dose levels and exposure probability

The low dose EnnB in this study correlates approximately with the highest observed levels of EnnB by IMRs surveillance (Sele et al., 2021). The highest levels observed in commercial salmon feeds observed in IMRs surveillance program was 25 µg/kg for Bea 250 µg/kg for EnnB (Sele et al., 2021). While highest estimated theoretical levels based on data from commercial fish feeds were 270 µg/kg for Bea and 6850 µg/kg for EnnB (Pietsch et al., 2020).

The lower benchmark dose model (BMDL) assessment in the present study was only preformed on the physiological parameter's that were significantly affected by the treatment, which were SGR and CF for Bea in addition to SGR and SLR for EnnB. The BMDL indicated safe dietary EnnB levels for SGR and SLR of 248 and 259 µg/kg, respectively. EnnB was also the mycotoxin of highest prevalence in samples in the surveillance program of IMR (Sele et al., 2021). Given that highest observed levels of EnnB within the same range as the presented BMDLs indicates a higher probability of salmon being exposed to harmful concentrations of EnnB through feed in aquaculture, in contrast to Bea. The safe dietary Bea levels indicate by BMDL was 321 and 511 µg/kg for SGR and CF, respectively. Which is well above the observed- and the theoretical highest level of exposure of Bea. Nevertheless, one might speculate if the BMDL based on solely on physiological performance would underestimate the risk involved in Bea contamination of feed. As deduced in the permeability measurements where Bea treatments showed a dose dependent increase, in which were low- (0.25 mg/kg) and high dose Bea (25 mg/kg) had a significant effect.

Although no transfer of EnnB or Bea has been recoded from fish to fillet exposing us at risk of exposure (Institute of Marine Research, 2021), the focus of fish welfare remains essential to be able to have a sustainable aquaculture production in the future. Accordingly, due to the observed contamination levels of EnnB especially, further characterization is essential to investigate chronic toxicity individually as well as potential combinatory effects, with other mycotoxins as in nature.

5. Conclusion

The present trial beauvericin caused a significant increase of apparent permeability without apparent histological effects and signs of inflammation in distal intestinal segments of Atlantic salmon. The increased intestinal permeability was most likely due to beauvericin's ionophoric capabilities, causing a disruption of cellular homeostasis. Accompanied by a decreasing condition factor and non-efficient feed conversion ratio. Implying an impaired ability to utilize the feed, a more direct effect on the intestine. By contrast, enniatin B had no effect on the apparent permeability in distal intestinal segments. Furthermore, more subtle effects on intestinal function were observed in enniatin treatments. Displayed by alterations in biomarkers of oxidative stress, cytokine signaling transduction and regulation of heme biosynthesis. As seen from low dose beauvericin treatment significantly upregulating both *ALAS1* and *Gpx4*. Also, low- and high dose enniatin B treatment significantly upregulated *MnSOD* and *SOCS2* respectively. In summary, indicating an effect of exposure in both EnnB and Bea treatments, however in different manners. The difference in results could be attributed to their minor but meaningful dissimilarities, resulting in a different degree of toxicity. In light of the above, EnnB and Bea poses a risk through salmon feed in aquaculture. Emphasizing the importance of further *in vivo* characterization of EnnB and Bea to establish safe dietary levels in salmon feed.

6. Future perspectives

The obtained result in the present study underlines the need of further characterization of EnnB and Bea in the future. Of both the mother compounds and their metabolites, to be able to perform adequate risk assessment and risk management. No *in vivo* study exposing Atlantic salmon to EnnB and Bea has previously been performed. In an ideal world with unlimited budget and resources, a chronic exposure would have been preferred to better understand the role of EnnB and Bea. Where also looking at possible toxicant-interactions would be desirable, giving a more comprehensive mapping of in vivo metabolism of EnnB and Bea. Additionally reflecting the realistic mycotoxin exposure trough feed in aquaculture, as mycotoxins frequently co-occur (Jonsson, 2017).

7. References

ANFOSSI, L., GIOVANNOLI, C. & BAGGIANI, C. 2016. Mycotoxin detection. *Current Opinion in Biotechnology,* 37**,** 120-126.

BERNHOFT, A., ERIKSEN, G. S., SUNDHEIM, L., BERNTSSEN, M., BRANTSÆTER, A. L., BRODAL, G., FÆSTE, C. K., HOFGAARD, I. S., RAFOSS, T., SIVERTSEN, T. & TRONSMO, A. 2013. Risk assessment of mycotoxins in cereal grain in Norway. *Opinion of the Scientific Steering Committee of the Norwegian Scientific Committee for Food Safety***,** 287.

BERNTSSEN, M. H. G., ROSENLUND, G., GARLITO, B., AMLUND, H., SISSENER, N. H., BERNHARD, A. & SANDEN, M. 2021. Sensitivity of Atlantic salmon to the pesticide pirimiphos-methyl, present in plant-based feeds. *Aquaculture,* 531**,** 735825.

BERTERO, A., MORETTI, A., SPICER, L. J. & CALONI, F. 2018. Fusarium Molds and Mycotoxins: Potential Species-Specific Effects. *Toxins,* 10**,** 244.

BURCHAM, P. C. 2014. *Introduction to Toxicology,* London, London: Springer London.

CAMPBELL, N. A., URRY, L. A., CAIN, M. L., WASSERMAN, S. A., MINORSKY, P. V. & REECE, J. B. 2018. *Biology : A global approach,* New York, Pearson Education.

COMMITTEE, E. S., HARDY, A., BENFORD, D., HALLDORSSON, T., JEGER, M. J., KNUTSEN, K. H., MORE, S., MORTENSEN, A., NAEGELI, H., NOTEBORN, H., OCKLEFORD, C., RICCI, A., RYCHEN, G., SILANO, V., SOLECKI, R., TURCK, D., AERTS, M., BODIN, L., DAVIS, A., EDLER, L., GUNDERT-REMY, U., SAND, S., SLOB, W., BOTTEX, B., ABRAHANTES, J. C., MARQUES, D. C., KASS, G. & SCHLATTER, J. R. 2017. Update: use of the benchmark dose approach in risk assessment. *EFSA Journal,* 15**,** e04658.

DA SILVA, E., BRACARENSE, A. P. & OSWALD, I. P. 2018. Mycotoxins and oxidative stress: where are we? *World Mycotoxin Journal,* 11**,** 113-134.

DAVIS, A., GRONDIN, C., JOHNSON, R., SCIAKY, D., WIEGERS, J., WIEGERS, T. & MATTINGLY, C. 2020. *The Comparative Toxicogenomics Database* [Online]. Available: http://ctdbase.org/detail.go?type=chem&acc=C100264 [Accessed 23.05.2022 2022].

ESCRIVÁ, L., FONT, G. & MANYES, L. 2015. In vivo toxicity studies of fusarium mycotoxins in the last decade: A review. *Food and Chemical Toxicology,* 78**,** 185-206.

FJELLDAL, P. G., LOCK, E.-J., GROTMOL, S., TOTLAND, G. K., NORDGARDEN, U., FLIK, G. & HANSEN, T. 2006. Impact of smolt production strategy on vertebral growth and mineralisation during smoltification and the early seawater phase in Atlantic salmon (Salmo salar, L.). *Aquaculture,* 261**,** 715-728.

GAD, S. C. 2007. *Toxicology of the gastrointestinal tract,* Boca Raton, CRC Press.

GAJĘCKA, M., STOPA, E., TARASIUK, M., ZIELONKA, Ł. & GAJĘCKI, M. 2013. The Expression of Type-1 and Type-2 Nitric Oxide Synthase in Selected Tissues of the Gastrointestinal Tract during Mixed Mycotoxicosis. *Toxins,* 5**,** 2281-2292.

GALARZA-SEEBER, R., LATORRE, J. D., BIELKE, L. R., KUTTAPPAN, V. A., WOLFENDEN, A. D., HERNANDEZ-VELASCO, X., MERINO-GUZMAN, R., VICENTE, J. L., DONOGHUE, A., CROSS, D., HARGIS, B. M. & TELLEZ, G. 2016. Leaky Gut and Mycotoxins: Aflatoxin B1 Does Not Increase Gut Permeability in Broiler Chickens. *Frontiers in Veterinary Science,* 3.

GAO, Y., MENG, L., LIU, H., WANG, J. & ZHENG, N. 2020. The Compromised Intestinal Barrier Induced by Mycotoxins. *Toxins,* 12**,** 619.

GRUBER-DORNINGER, C., JENKINS, T. & SCHATZMAYR, G. 2019. Global mycotoxin occurrence in feed: A ten-year survey. *Toxins,* 11**,** 375.

GUERRE, P. 2020. Mycotoxin and Gut Microbiota Interactions. *Toxins,* 12**,** 769.
HUMAN, U. 2019. Biomin World Mycotoxin Survey 2018. *AFMA Matrix.*

INSTITUTE OF MARINE RESEARCH 2021. Annual report for samples retrieved in 2020. *Monitoring program for fish feed.* Bergen: Institute of Marine Research.

JONSSON, M. 2017. *The toxicity of Fusarium mycotoxins enniatin and moniliformin.* PhD, University of Helsinki.

KAUSHIK, S. J. & MÉDALE, F. 1994. Energy requirements, utilization and dietary supply to salmonids. *Aquaculture,* 124**,** 81-97.

KNUDSEN, D., JUTFELT, F., SUNDH, H., SUNDELL, K., KOPPE, W. & FRØKIÆR, H. 2008. Dietary soya saponins increase gut permeability and play a key role in the onset of soyabean-induced enteritis in Atlantic salmon (Salmo salar L.). *British Journal of Nutrition,* 100**,** 120-129.

KNUDSEN, D., URÁN, P., ARNOUS, A., KOPPE, W. & FRØKIÆR, H. 2007. Saponin-Containing Subfractions of Soybean Molasses Induce Enteritis in the Distal Intestine of Atlantic Salmon. *Journal of Agricultural and Food Chemistry,* 55**,** 2261-2267.

KO, C.-W., QU, J., BLACK, D. D. & TSO, P. 2020. Regulation of intestinal lipid metabolism: current concepts and relevance to disease. *Nature Reviews Gastroenterology & Hepatology,* 17**,** 169-183.

KOUADIO, J. H., DANO, S. D., MOUKHA, S., MOBIO, T. A. & CREPPY, E. E. 2007. Effects of combinations of Fusarium mycotoxins on the inhibition of macromolecular synthesis, malondialdehyde levels, DNA methylation and fragmentation, and viability in Caco-2 cells. *Toxicon,* 49**,** 306-317.

KRUG, I., BEHRENS, M., ESSELEN, M. & HUMPF, H.-U. 2018. Transport of enniatin B and enniatin B1 across the blood-brain barrier and hints for neurotoxic effects in cerebral cells. *PloS one,* 13**,** e0197406.

LEITGEB, R., RAFFASEDER, C., RUCKENBAUER, P., LEMMENS, M., BÖHM, J., WAGNER, E., KRSKA, R. & PARICH, A. 2003. Impact of Fusarium toxins on growth and slaughter performance of broilers and turkeys. *Mycotoxin Research,* 19**,** 180-184.

LIEW, W. P. P. & MOHD-REDZWAN, S. 2018. Mycotoxin: Its Impact on Gut Health and Microbiota. *Frontiers in Cellular and Infection Microbiology,* 8.

LIU, Y., OLAF OLAUSSEN, J. & SKONHOFT, A. 2011. Wild and farmed salmon in Norway—A review. *Marine Policy,* 35**,** 413-418.

LØKKA, G., AUSTBØ, L., FALK, K., BJERKÅS, I. & KOPPANG, E. O. 2013. Intestinal morphology of the wild Atlantic salmon (Salmo salar). *Journal of morphology,* 274**,** 859-876.

MARANGHI, F., TASSINARI, R., NARCISO, L., TAIT, S., ROCCA, C. L., FELICE, G. D., BUTTERONI, C., CORINTI, S., BARLETTA, B. & CORDELLI, E. 2018. In vivo toxicity and genotoxicity of beauvericin and enniatins. Combined approach to study in vivo toxicity and genotoxicity of mycotoxins beauvericin (BEA) and enniatin B (ENNB). *EFSA Supporting Publications,* 15**,** 1406E.

MARROQUÍN-CARDONA, A. G., JOHNSON, N. M., PHILLIPS, T. D. & HAYES, A. W. 2014. Mycotoxins in a changing global environment – A review. *Food and Chemical Toxicology,* 69**,** 220-230.

MATEER, S. W., CARDONA, J., MARKS, E., GOGGIN, B. J., HUA, S. & KEELY, S. 2016. Ex vivo intestinal sacs to assess mucosal permeability in models of gastrointestinal disease. *JoVE (Journal of Visualized Experiments)***,** e53250.

MCCORMICK, S. D. 2012. Smolt Physiology and Endocrinology. *In:* MCCORMICK, S. D., FARRELL, A. P. & BRAUNER, C. J. (eds.) *Fish Physiology.* Academic Press.

MCLAUGHLIN, J., LAMBERT, D., PADFIELD, P. J., BURT, J. P. H. & O'NEILL, C. A. 2009. The mycotoxin patulin, modulates tight junctions in caco-2 cells. *Toxicology in Vitro,* 23**,** 83-89.

MOLDAL, T., BERNHOFT, A., ROSENLUND, G., KALDHUSDAL, M. & KOPPANG, E. O. 2018. Dietary Deoxynivalenol (DON) May Impair the Epithelial Barrier and Modulate the Cytokine Signaling in the Intestine of Atlantic Salmon (Salmo salar). *Toxins,* 10**,** 376.

NIMALAN, N., SØRENSEN, S. L., FEČKANINOVÁ, A., KOŠČOVÁ, J., MUDROŇOVÁ, D.,

GANCARČÍKOVÁ, S., VATSOS, I. N., BISA, S., KIRON, V. & SØRENSEN, M. 2022. Mucosal barrier status in Atlantic salmon fed marine or plant-based diets supplemented with probiotics. *Aquaculture,* 547**,** 737516.

NORWEGIAN FOOD SAFETY AUTHORITY 2019. Anbefalte Grenseverdier for sopp og Mykotoksiner in Fôrvarer. Oslo, Norway: Norwegian Food Safety Authority.

NORWEGIAN FOOD SAFETY AUTHORITY. 2020. *Regelverk om muggsoppgifter i mat* [Online]. Norwegian Food Safety Authority. Available: https://www.mattilsynet.no/mat_og_vann/uonskede_stofferimaten/biologiske_gifter/muggsoppgifter/regelverk_om_muggsoppgifter_i_mat.9328 [Accessed 18.05.2022 2022].

NORWEGIAN SEAFOOD RESEARCH FUND. 2017. *Kartlegging og forbedring av tarmhelsen hos oppdrettslaks (GutMatters)* [Online]. Available: https://www.fhf.no/prosjekter/prosjektbasen/901435/ [Accessed 30.05.2022 2022].

NOVAK, B., LOPES HASUDA, A., GHANBARI, M., MAYUMI MARUO, V., BRACARENSE, A. P. F. R. L., NEVES, M., EMSENHUBER, C., WEIN, S., OSWALD, I. P., PINTON, P. & SCHATZMAYR, D. 2021. Effects of Fusarium metabolites beauvericin and enniatins alone or in mixture with deoxynivalenol on weaning piglets. *Food and Chemical Toxicology,* 158**,** 112719.

OLSVIK, P. A., KROGLUND, F., FINSTAD, B. & KRISTENSEN, T. 2010. Effects of the fungicide azoxystrobin on Atlantic salmon (Salmo salar L.) smolt. *Ecotoxicology and Environmental Safety,* 73**,** 1852-1861.

PAHLOW, M., VAN OEL, P. R., MEKONNEN, M. M. & HOEKSTRA, A. Y. 2015. Increasing pressure on freshwater resources due to terrestrial feed ingredients for aquaculture production. *Science of The Total Environment,* 536**,** 847-857.

PROSPERINI, A., BERRADA, H., RUIZ, M. J., CALONI, F., COCCINI, T., SPICER, L. J., PEREGO, M. C. & LAFRANCONI, A. 2017. A Review of the Mycotoxin Enniatin B. *Frontiers in Public Health,* 5.

RAŠKOVIĆ, B., STANKOVIĆ, M., MARKOVIĆ, Z. & POLEKSIĆ, V. 2011. Histological methods in the assessment of different feed effects on liver and intestine of fish. *Journal of Agricultural Sciences (Belgrade),* 56**,** 87-100.

ROBERTS, M. S., MAGNUSSON, B. M., BURCZYNSKI, F. J. & WEISS, M. 2002. Enterohepatic Circulation. *Clinical Pharmacokinetics,* 41**,** 751-790.

RODRÍGUEZ-CARRASCO, Y., HEILOS, D., RICHTER, L., SÜSSMUTH, R. D., HEFFETER, P., SULYOK, M., KENNER, L., BERGER, W. & DORNETSHUBER-FLEISS, R. 2016. Mouse tissue distribution and persistence of the food-born fusariotoxins Enniatin B and Beauvericin. *Toxicology Letters,* 247**,** 35-44.

RUIJTER, J., RAMAKERS, C., HOOGAARS, W., KARLEN, Y., BAKKER, O., VAN DEN HOFF, M. & MOORMAN, A. 2009. Amplification efficiency: linking baseline and bias in the analysis of quantitative PCR data. *Nucleic acids research,* 37**,** e45-e45.

SANTINI, A., MECA, G., UHLIG, S. & RITIENI, A. 2012. Fusaproliferin, beauvericin and enniatins: occurrence in food–a review. *World Mycotoxin Journal,* 5**,** 71-81.

SØDERSTRØM, S., LIE, K. K., LUNDEBYE, A.-K. & SØFTELAND, L. 2022. Beauvericin (BEA) and enniatin B (ENNB)-induced impairment of mitochondria and lysosomes-Potential sources of intracellular reactive iron triggering ferroptosis in Atlantic salmon primary hepatocytes. *Food and Chemical Toxicology***,** 112819.

SØRENSEN, S. L., PARK, Y., GONG, Y., VASANTH, G. K., DAHLE, D., KORSNES, K., PHUONG, T. H., KIRON, V., ØYEN, S. & PITTMAN, K. 2021. Nutrient Digestibility, Growth, Mucosal Barrier Status, and Activity of Leucocytes From Head Kidney of Atlantic Salmon Fed Marine-or Plant-Derived Protein and Lipid Sources. *Frontiers in immunology,* 11**,** 3939.

TEDJIOTSOP FEUDJIO, F., DORNETSHUBER, R., LEMMENS, M., HOFFMANN, O., LEMMENS-GRUBER, R. & BERGER, W. 2010. Beauvericin and enniatin: emerging toxins and/or remedies? *World Mycotoxin Journal,* 3**,** 415-430.

TIPSMARK, C. K., SØRENSEN, K. J., HULGARD, K. & MADSEN, S. S. 2010. Claudin-15 and -25b expression in the intestinal tract of Atlantic salmon in response to seawater acclimation, smoltification and hormone treatment. *Comparative Biochemistry and Physiology Part A: Molecular & Integrative Physiology,* 155**,** 361-370.

TONSHIN, A. A., TEPLOVA, V. V., ANDERSSON, M. A. & SALKINOJA-SALONEN, M. S. 2010. The Fusarium mycotoxins enniatins and beauvericin cause mitochondrial dysfunction by affecting the mitochondrial volume regulation, oxidative phosphorylation and ion homeostasis. *Toxicology,* 276**,** 49-57.

VANDESOMPELE, J., DE PRETER, K., PATTYN, F., POPPE, B., VAN ROY, N., DE PAEPE, A. & SPELEMAN, F. 2002. Accurate normalization of real-time quantitative RT-PCR data by geometric averaging of multiple internal control genes. *Genome Biology,* 3.

WU, Q., PATOCKA, J., NEPOVIMOVA, E. & KUCA, K. 2018. A Review on the Synthesis and Bioactivity Aspects of Beauvericin, a Fusarium Mycotoxin. *Frontiers in Pharmacology,* 9.

XIA, X., CHENG, Z., HE, B., LIU, H., LIU, M., HU, J., LEI, L., WANG, L. & BAI, Y. 2021. Ferroptosis in aquaculture research. *Aquaculture,* 541**,** 736760.

AAS, T. S., YTRESTØYL, T. & ÅSGÅRD, T. 2019. Utilization of feed resources in the production of Atlantic salmon (Salmo salar) in Norway: An update for 2016. *Aquaculture Reports,* 15**,** 100216.

Appendix A

Table A1: Chemicals utilized in this thesis

Name	Supplier
Toludine blue	Sigma-Aldrich
RNase inhibitor	
Ethanol 96%	Antibac
GelRed	Biotium
RNA 6000 Ladder	Invitrogen
Entellan ®	Kulzer
Qiazol Lysis Reagent	Qiagen
GelPilot 50 bp Ladder	Qiagen
RNase inhibitor	Qiagen
RNase-Free DNase Set	Qiagen
TE buffer	PanReac AppliChem
LightCycler® 480 SYBR Green I Master	Roche
Formaldehyde 37%	Sigma-Aldrich
Phosphate- buffered saline (PBS)	Sigma-Aldrich
Fluorescein isothiocyanate–dextran (MW 4000)	Sigma-Aldrich

Table A2: Commercial kits utilized in this thesis

Kit	Supplier
RNA 6000 Nano Kit	Agilent
TaqMan Reverse Transcriptase reagents	Applied biosystems
Technovit 7100 ®	Kulzer
Technovit 3040 ®	Kulzer
OneStep RT-PCR kit	Quiagen
EZ1 RNA Tissue Mini Kit	Quiagen

Table A3: Equipment utilized in this thesis

Equipment/instrument	Supplier	Application
Histoblock	Kulzer	Block for mold
PCR Plate, 96-well, non-skirted	Thermo Fisher	cDNA
MicroAmp™ 96-well Full Plate Cover	Applied Biosystems	cDNA
Histoform	Kulzer	Embedding mold
Chip priming station	Agilent	Loading nano chip
MicroAmp™ Adhesive Film Applicator	Applied Biosystems	qPCR
MicroAmp™ Optical Adhesive Film	Applied Biosystems	qPCR
96 well plate	VWR	qPCR
LightCycler ® 480 Multiwell Plate 384	Roche	qPCR
RNA chip	Agilent	Separate nucleic acid fragments

Table A4: Instruments utilized in this thesis

Instrument	Supplier	Application
Centrifuge 5804R	Eppendorf	Centrifuge
Mini-Protean ® Tetra System	Bio-Rad	Electrophoresis
Power Pac 2000	Bio-Rad	Electrophoresis
Chemidoc XRS+	Bio-Rad	Gel doc
GeneAmp PCR 9700	Termo Fisher	Gene amplification
Block Heater SBH130DC	Stuart	Heatingblock
Precellys 24 Tissue Homogenizer	Bertin Instruments	Homogenization
Micro Star 17R	VMR	Microcentrifuge
Nikon Eclipse E200	Nikon	Microscope
Biomek 4000	Beckman coulter	Pipetting robot
Mixmate	Eppendorf	Platecentrifuge
Victor X5 2030 Multilabel reader	PerkinElmer	Platereader
CFX384 Touch Real-Time PCR Detection System	Bio-Rad	qPCR
Light Cycler ® 480 Instrument	Roche	qPCR
Bio robot EZ1	Qiagen	RNA purification
2100 Bioanalyzer	Agilent	RNA quality
Chip priming station	Agilent Life	RNA quality
Nano drop	Termo Fisher	RNA quantitation
Leica RM2165	Leica	Rotary microtome
NanoZoomer® S60	Hamamatsu	Slide image scanner
Slide warmer SW 85	Leica	Slide warmer
Hetofrig CB11	Heto Inter med	Temperature bath
MS 3 s36 Basic Chip Vortex	IKA	Vortex

Table A5: Software utilized in this thesis

Software	Supplier
2100 Bioanalyzer Expert Software	Agilent
Image Lab ™ 6.0.1	Bio-Rad
Bio-Rad CFX Maestro	Bio-Rad
Graph Pad Prism 9.3.0	Gaph Pad Software Inc.
NDP®.view2. Image viewing software	Hamamatsu
Nanodrop	Isogen Life Science
Excel	Microsoft
Word (v2022)	Microsoft
ImageJ	National Institutes of Health
PerkinElmer 2030 Software version 4.00	PerkinElmer
ChemDraw	CambridgeSoft.

Appendix B

Table B1: Components in Toluidine Blue mix

Component	Volume
Toluidine blue O	1 g
Sodium Borate (Borax)	1 g
Milli Q water	100 ml

Table B2: QIAGEN OneStep reaction mix and RT-PCR reaction conditions

Reaction mix	25µl rxn	RT-PCR reaction conditions			
5x QIAGEN OneStep RT-PCR buffer	5 µl	Reverse transcriptase	30 min	50°C	
Q solution	5 µl	PCR activation	15 min	95°C	
dNTP mix	1 µl	Denaturation	45 sek	94°C	x 35
Primer forward	0,5 µl	Annealing	45 sek	60°C	
Primer reverse	0,5 µl	Extension	1 min	72°C	
RNase inhibitor	0,25 µl	Final extension	10 min	72°C	
5x QIAGEN OneStep RT-PCR Enzyme mix	1 µl				
RNase free water	-				
Template RNA	-				

Table B3 cDNA reaction mix for 50 µl cDNA reaction (40 µl mix + 10 µl RNA)

Component	50 µl	Final concentration (mM)
H_2O free from RNase	8.9	
10X TaqMan RT buffer	5.0	1X
25 mM magnesium chloride	11.0	5.5mM
10 mM deoxyNTPs mixture	10.0	500 µM per dNTP
50 µM oligo $d(T)_{16}$	2.5	2.5 µM
RNase inhibitor	1.0	0.4 U/µl
Multiscribe Reverse transcriptase	1.67	1.67 U/ µl

Table B4: Reverse transcriptase reaction-conditions

Step	Incubation	RT	Reverse transcriptase inactivation	End
Temperature (°C)	25	48	95	4
Time (minutes)	10	60	5	∞
Volume (µl)	50			

Table B5: SYBRGreen reaction mix for Light Cycler 480

Reagent	Volume per sample (µl)	Final concentration
Milli Q water	2.8	
Primer I	0.1	500 nM
Primer II	0.1	500 nM
SYBRGreen PCR Master Mix (x2)	5	1X

Table B6: Real-time PCR reaction conditions

Step	Preincubation	Amplification			Melting point analysis			Cooling
Temperature (°C)	95	95	60	72	95	65	97	40
Time	5m	10s	10s	10s	5s	1m		10s
Number of cycles	1	45			1			
Volume (µl)	20							

Table B7. Components in Ringers' solution

Component	Concentration (mM)
Magnesium chloride	0.47
Potassium chloride	2.5
Sodium bicarbonate	20.2
Monosodium phosphate	0.42
Calcium chloride	1.5
Sodium chloride	129

Table B8. Fluorescein isothiocyanate–dextran [0.5 mg/mL]

Component	Volume
Fluorescein isothiocyanate–dextran (MW 4000)	10 mg
Ringers´solution (Table B7)	20 mL

Appendix C

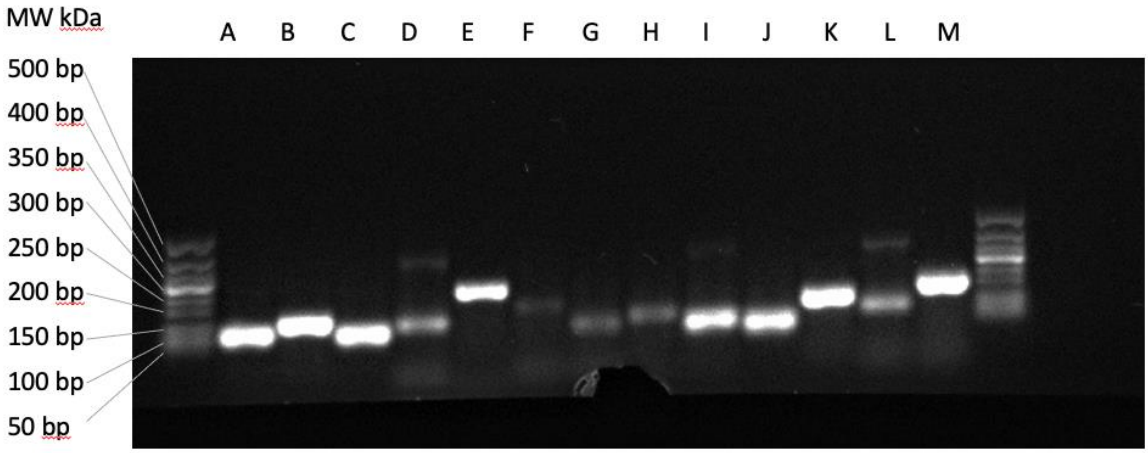

Figure C1: Primers tested using OneStep RT-PCR and 1% agarose gel. A mix of all RNA samples were utilized as template for the PCR reaction, with GelPilot 50 bp as standard. Gel depicted in Chemidoc XRS+ systems in combination with software Image Lab ™. Primes; A = *ALAS1*_F1, B = *ALAS1*_F2, C = OCLN, D = Hprt, E = SOCS1_1, F =*SOCS2*_2, G = Cx32.2, H = ALAS2, I = CLDN25b, J = ATP8 , K = PCNA , L = Kpca1 , M = *SOCS2*_1.

Appendix D

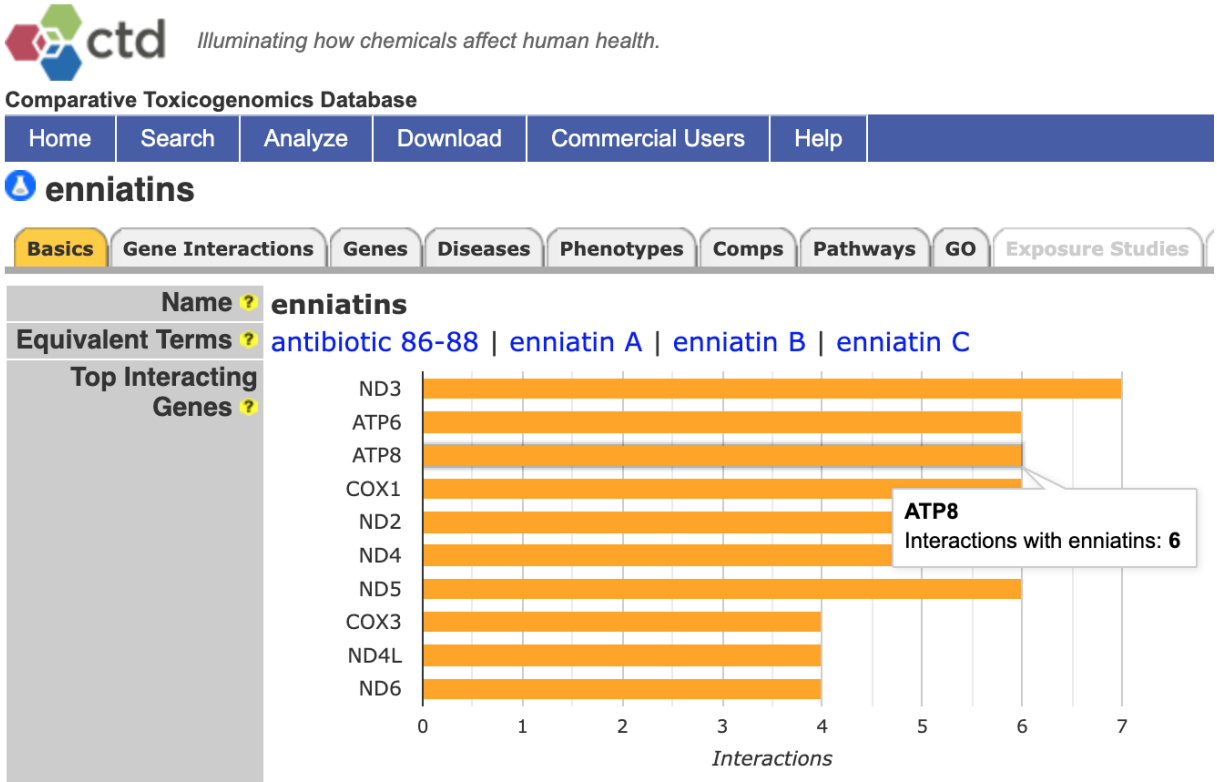

Figure D1: Illustration of ATP8 being amongst the top interacting genes (9 interactions) with enniatins. DAVIS, A., GRONDIN, C., JOHNSON, R., SCIAKY, D., WIEGERS, J., WIEGERS, T. & MATTINGLY, C. 2020. The Comparative Toxicogenomics Database [Online]. Available: http://ctdbase.org/detail.go?type=chem&acc=C100264 [Accessed 23.05.2022 2022].

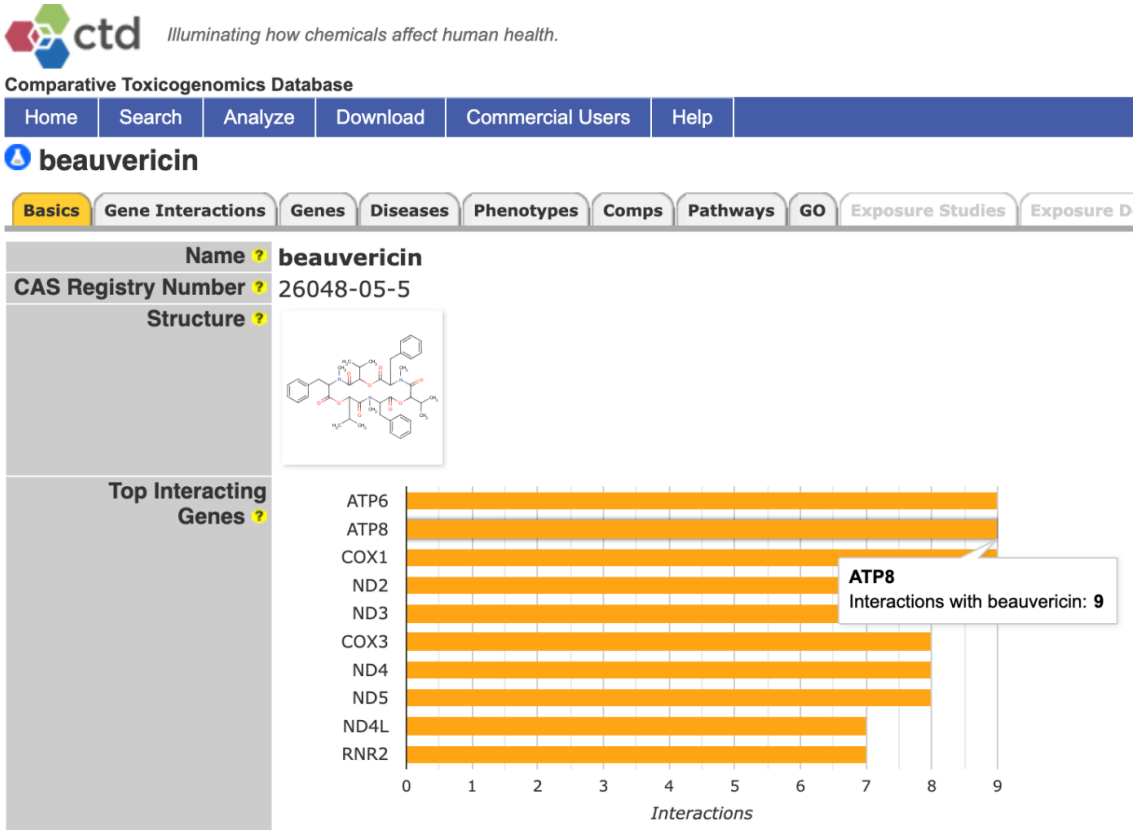

Figure D2: Illustration of ATP8 being amongst the top interacting genes (9 interactions) with beauvericin. DAVIS, A., GRONDIN, C., JOHNSON, R., SCIAKY, D., WIEGERS, J., WIEGERS, T. & MATTINGLY, C. 2020. The Comparative Toxicogenomics Database [Online]. Available: http://ctdbase.org/detail.go?type=chem&acc=C004456 [Accessed 23.05.2022 2022].